General Disclaimer

One or more of the Following Statements may affect this Document

- This document has been reproduced from the best copy furnished by the organizational source. It is being released in the interest of making available as much information as possible.

- This document may contain data, which exceeds the sheet parameters. It was furnished in this condition by the organizational source and is the best copy available.

- This document may contain tone-on-tone or color graphs, charts and/or pictures, which have been reproduced in black and white.

- This document is paginated as submitted by the original source.

- Portions of this document are not fully legible due to the historical nature of some of the material. However, it is the best reproduction available from the original submission.

ENSCO, Inc.
1980 N. Atlantic Ave., Suite 230
Coca Beach, FL 32931
(321) 783-9735, (321) 853-8202 (AMU)

Applied Meteorology Unit (AMU) Quarterly Report

Third Quarter FY-07 Contract NNK06MA70C 31 July 2007

Distribution:

NASA HQ/M/AA/W. Gerstenmaier
NASA KSC/AA/W. Parsons
NASA KSC/MK/L. Cain
NASA KSC/LX/J. Talone
NASA KSC/PH/ R. Willcoxon
NASA KSC/PH-A2/D. Lyons
NASA KSC/PH/M. Leinbach
NASA KSC/PH/S. Minute
NASA KSC/VA/S. Francois
NASA KSC/VA-2/C. Dovale
NASA KSC/KT/D. Bartine
NASA KSC/KT-C/R. Nelson
NASA KSC/KT-C-H/J. Madura
NASA KSC/KT-C-H/F. Merceret
NASA KSC/KT-C-H/J. Ward
NASA JSC/MA/W. Hale
NASA JSC/MS2/C. Boykin
NASA JSC/WS8/F. Brody
NASA JSC/WS8/R. Lafosse
NASA JSC/WS8/B. Hoeth
NASA JSC/WS8/S. Early
NASA MSFC/EV13/D. Edwards
NASA MSFC/EV13/B. Roberts
NASA MSFC/EV13/S. Deaton
NASA MSFC/EV13/R. Decker
NASA MSFC/MP71/G. Overbey
NASA MSFC/SPoRT/W. Lapenta
NASA DFRC/RA/E. Teets
NASA LaRC/M. Kavaya
45 WS/CC/A. Boerlage
45 WS/DO/M. Gauthier
45 WS/DOU/M. McAleenan
45 WS/DOR/K. Nordgren
45 WS/DOR/P. Phan
45 WS/DOR/F. Flinn
45 WS/DOR/ T. McNamara
45 WS/DOR/J. Tumbiolo
45 WS/DOR/K. Winters
45 WS/SYA/B. Boyd
45 WS/SYR/W. Roeder
45 RMS/CC/M. Wasson
45 RMS/LGP/R. Fore
45 SW/SESL/D. Berlinrut
45 SW/XPR/R. Hillyer
45 OG/CC/D. Thompson
CSR 4500/H. Herring
CSR 7000/M. Maier
SMC/RNP/S. Exum
SMC/RNP/T. Knox
SMC/RNP/R. Bailey
SMC/RNP (PRC)/K. Spencer
HQ AFSPC/A3FW/J. Carson
HQ AFWA/DN/M. Surmeier
HQ AFWA/DNXT/G. Brooks
HQ AFWA/XOR/M. Treu
HQ USAF/XOW/J. Murphy
HQ USAF/A30-WX/M. Zettlemoyer
NOAA "W/NP"/L. Uccellini
NOAA/OAR/SSMC-I/J. Golden
NOAA/NWS/OST12/SSMC2/J. McQueen
NOAA Office of Military Affairs/M. Babcock
NWS Melbourne/B. Hagemeyer
NWS Melbourne/D. Sharp
NWS Melbourne/S. Spratt
NWS Melbourne/P. Blottman
NWS Melbourne/M. Volkmer

Continued on Page 2

Executive Summary

This report summarizes the Applied Meteorology Unit (AMU) activities for the second quarter of Fiscal Year 2007 (January - March 2007). A detailed project schedule is included in the Appendix.

Task — Objective Lightning Probability Tool: Phase II

Goal Update the lightning probability forecast equations used in 45th Weather Squadron (45 WS) operations with new data and create a graphical user interface (GUI) in the Meteorological Interactive Data Display System (MIDDS) that automatically gathers the data needed as input to the equations developed in Phase I of this task. The new data may improve the performance of the equations, and the automated tool will increase forecaster efficiency.

Milestones Updated the Excel GUI that was developed in Phase I, and created a new GUI in MIDDS. Both GUIs were delivered to operations.

Discussion The design and function of new MIDDS GUI is similar to the Excel GUI, making the transition to using the new GUI much easier for forecasters. It goes a step further than the Excel GUI by accessing the date and stability parameters automatically for input to the equations. This reduces the probability of human error and eliminates the time forecasters would spend looking up the values, allowing them to do other important functions.

Task — Peak Wind Tool for General Forecasting

Goal Develop a tool to forecast the peak wind speed for the day from the surface to 300 ft on Kennedy Space Center (KSC)/Cape Canaveral Air Force Station (CCAFS) during the cool season (October – April). The tool should be able to forecast the timing of the peak wind speed and the background average wind speed, based on observational data available for the 45 WS 0700L weather briefing.

Milestones Developed equations to predict the daily peak wind speed, the timing of the peak, and the average wind speed at the time of the peak. The first version of GUI that forecasters will use to interact with the equations and display the predicted winds was created.

Discussion Tower, surface, and upper-air observations for the cool season months from October 2002 to February 2007 were used to create equations to predict the daily peak wind and average wind at KSC and CCAFS. An Excel application with a GUI was developed to display the predicted winds. Based on a review by the 45 WS, the application is being updated to combine the prediction equations and display the probability of the peak wind exceeding 34, 49, and 59 kt.

Continued on Page 2

Distribution (continued from Page 1)

NWS Southern Region HQ/"W/SR"/ S. Cooper
NWS Southern Region HQ/"W/SR3" D. Billingsley
NWS/"W/OST1"/B. Saffle
NWS/"W/OST12"/D. Melendez
NSSL/D. Forsyth
30 WS/DO/J. Kurtz
30 WS/DOR/M. Barnhill
30 WS/DOR/S Storr
30 WS/SY/M. Schmeiser
30 WS/SYR/G. Davis
30 WS/SYR/D Vorhees
30 WS/SYS/J. Mason
30 SW/XPE/R. Ruecker
Det 3 AFWA/WXL/K. Lehneis
NASIC/FCTT/G. Marx
46 WS//DO/J. Mackey
46 WS/WST/C. Chase
412 OSS/OSWM/P. Harvey
UAH/NSSTC/W. Vaughan
FAA/K. Shelton-Mur
FSU Department of Meteorology/H. Fuelberg
ERAU/Applied Aviation Sciences/ C. Herbster
ERAU/CAAR/I. Wilson
NCAR/J. Wilson
NCAR/Y. H. Kuo
NOAA/FRB/GSD/J. McGinley
NOAA/FRB/GSD/S. Koch
Office of the Federal Coordinator for Meteorological Services and Supporting Research/R. Dumont
Boeing Houston/S. Gonzalez
Aerospace Corp/T. Adang
ACTA, Inc./B. Parks
ITT/G. Kennedy
Timothy Wilfong & Associates./T. Wilfong
ENSCO, Inc./E. Lambert
ENSCO, Inc./A. Yersavich
ENSCO, Inc./S. Masters

Executive Summary, *continued*

Task — Situational Lightning Climatologies for Central Florida, Phase II

Goal — Create the climatological probability of lightning occurrence and mean number of strikes for each flow regime as in Phase I for the two 12-hour periods 0000–1200 and 1200–2400 UTC, and in 5-, 10-, 20-, and 30-n mi circles surrounding the Shuttle Landing Facility (SLF) in 1-, 3-, and 6-hour increments. The 12-hour climatologies will be used by the forecasters at the National Weather Service in Melbourne, FL (NWS MLB) to update their daily lightning threat index map. The SLF climatologies will aid in the aviation forecast requirements at NWS MLB, and provide a tool to the Spaceflight Meteorology Group (SMG) to assist them in making forecasts for Flight Rule violations of lightning occurrence during a shuttle landing.

Milestones — Developed and delivered the climatological values for each time interval, range ring, and flow regime at nine sites in a Hypertext Markup Language (HTML)-based GUI.

Discussion — The final part of this task, to develop climatologies for 5-, 10-, 20- and 30-n mi range rings at the SLF, was completed. Similar climatologies were completed for eight other airports in east-central Florida. The climatology values were displayed in tables and graphs, which were built into an HTML-based GUI. The final report is being written.

Task — Anvil Threat Corridor Forecast Tool in AWIPS

Goal — Migrate the Anvil Threat Corridor Forecast Tool from MIDDS to the Advanced Weather Interactive Processing System (AWIPS). This tool is used in launch and landing operations to determine the threat from natural or triggered lightning due to flight through anvil cloud. The SMG is depending more on AWIPS for operations and the 45 WS may replace MIDDS with AWIPS. The 45 WS and SMG requested that the AMU transition the anvil tool to AWIPS to ensure it will remain available for operations.

Milestones — The User's Guide, final report, and software were delivered to the customers. The tool is being used operationally.

Discussion — The User's Guide and the final report were reviewed by SMG and 45 WS. The documents were distributed to the AMU's customers after addressing the comments from the reviews, and it was added to the AMU website. The software and installation instructions for the Anvil Forecast Tool were also sent to SMG and 45 WS.

Continued on Page 3

Executive Summary, *continued*

Task	Volume Averaged Height Integrated Radar Reflectivity (VAHIRR)
Goal	Transition the VAHIRR algorithm into operations using Weather Surveillance Radar 1988 Doppler (WSR-88D) data. The previous lightning launch commit criteria (LLCC) for anvil clouds to avoid triggered lightning were restrictive and lead to unnecessary launch delays and scrubs. The VAHIRR algorithm was developed as a result of the Airborne Field Mill program as part of a new LLCC for anvil clouds. This algorithm will assist forecasters in providing fewer missed launch opportunities with no loss of safety compared with the previous LLCC.
Milestones	The software was updated to take into account the radar cone of silence, change the methodology of calculating cloud thickness, and account for the radar elevation in the calculation of the height and thickness of clouds. The test plan and test procedure documents were updated as a result of the software updates.
Discussion	The test plan and test procedure documentation are being reviewed. After the review, the test procedures will be conducted.

Task	Tower Data Skew-T Tool
Goal	The rapid reduction in visibility and ceiling associated with marine incursions is a concern to 30th Weather Squadron (30 WS) forecasters during launch operations at Vandenberg Air Force Base (VAFB). Such conditions are a launch safety concern for new launch vehicles that require they be viewable by remote cameras until radar lock-on. The 30 WS developed the Tower Data Skew-T Tool to help monitor the progress of marine-layer incursions. The AMU will evaluate the effectiveness of this tool for the 30 WS.
Milestones	Compared temperature and dew point temperature profiles from soundings and wind towers on VAFB from data collected during 10–21 August 2006. Began writing the final memorandum.
Discussion	Results from the tower temperature and dew point temperature composite profiles and VAFB rawinsonde comparisons indicate that it is best to use the tower profiles as a monitoring tool for moisture advection and lower-atmospheric cooling during the evening and early morning hours.

Continued on Page 4

TABLE of CONTENTS

Executive Summary, *continued*

Task: Weather Research and Forecasting (WRF) Model Sensitivity Study

Goal: Conduct several WRF sensitivity case studies to determine the best configuration to use operationally at SMG and NWS MLB for predicting warm season convective initiation. Determining the best model configuration will assist forecasters in their short-term thunderstorm forecasting for the general public and evaluating flight rules and launch commit criteria.

Milestones: Completed the model verification studies for all Local Analysis and Prediction System (LAPS)-Advanced Regional WRF (ARW), LAPS-Non-hydrostatic Mesoscale Model (NMM), and Advanced Regional Prediction System (ARPS) Data Analysis System (ADAS)-ARW model runs. Completed the verification for all local high-resolution nested (two-way, one-way, and no nest) model runs using LAPS/ARW. Wrote a first draft of the final report.

Discussion: All WRF model configurations over-predicted precipitation in the early hours of the forecast, indicating a model spin-up issue. Both LAPS-ARW and ADAS-ARW over-predicted rainfall throughout the forecast, while LAPS-NMM under-predicted rainfall. Based on a subjective evaluation, the LAPS-ARW slightly outperformed both ADAS-ARW and LAPS-NMM for predicting warm season convection. Based on this, the AMU recommends LAPS-ARW for operational use, but does not recommend a specific nested configuration since the forecasts were nearly identical between the one-way, two-way, and no-nest configurations.

Special Notice to Readers

Applied Meteorology Unit (AMU) Quarterly Reports are now available on the Wide World Web (www) at Hhttp://science.ksc.nasa.gov/amu/H.

The AMU Quarterly Reports are also available in electronic format via email. If you would like to be added to the email distribution list, please contact Ms. Winifred Lambert (321-853-8130, Hlambert.winifred@ensco.comH). If your mailing information changes or if you would like to be removed from the distribution list, please notify Ms. Lambert or Dr. Francis Merceret (321-867-0818, HFrancis.J.Merceret@nasa.govH).

Background

The AMU has been in operation since September 1991. Tasking is determined annually with reviews at least semi-annually. The progress being made in each task is discussed in this report with the primary AMU point of contact reflected on each task.

AMU ACCOMPLISHMENTS DURING THE PAST QUARTER

SHORT-TERM FORECAST IMPROVEMENT

Objective Lightning Probability Tool: Phase II (Ms. Lambert)

The 45th Weather Squadron (45 WS) forecasters include a probability of lightning occurrence in their daily morning briefings. This information is used by personnel involved in determining the possibility of violating launch commit criteria (LCC), evaluating flight rules (FR), and planning for daily ground operation activities on Kennedy Space Center (KSC) and Cape Canaveral Air Force Station (CCAFS). The AMU developed a set of logistic regression equations that calculate the probability of cloud-to-ground (CG) lightning occurrence in Phase I of this task (Lambert and Wheeler 2005). These equations outperformed several standard forecast methods used in operations. The graphical user interface (GUI) developed in Phase I allows forecasters to interface with the equations by entering parameter values to output a probability of lightning occurrence. The forecasters must gather data from the morning sounding and other sources, then manually input that data into the GUI. The 45 WS requested that a tool be developed on the Meteorological Interactive Data Display System (MIDDS) that retrieves the required parameter values automatically for the equations to calculate the probability of lightning for the day. This will reduce the possibility of human error and increase efficiency, allowing forecasters to do other duties. The 45 WS requested the AMU to add the warm season data from the years 2004 and 2005 to the Phase I 15-year 1989–2003 data set. They also requested modifications to the predictors in the hope of improving equation accuracy.

Excel and MIDDS GUIs

Ms. Lambert updated the GUI developed in Phase I (Lambert and Wheeler 2005) with the new equations and delivered it to the 45 WS and the Spaceflight Meteorology Group (SMG) after testing to ensure proper performance. Mr. Wahner of Computer Sciences Raytheon (CSR) built a GUI using the Tool Command Language (Tcl)/Toolkit (Tk) capability in MIDDS. The design and function of this GUI is similar to the Excel GUI. It has two dialog boxes: the first asks for equation input, and the second displays the equation output. It goes one step further by gathering the necessary sounding parameter values and entering them automatically into the dialog box. This removes the risk of a forecaster entering an incorrect value while also reducing the time the forecaster would spend gathering and calculating the required parameter values.

Ms. Lambert tested the MIDDS GUI by comparing its output to that of the updated Excel GUI. Both tools produced identical probability values with identical input. Mr. Wahner installed the tool on the MIDDS stations in 45 WS Range Weather Operations in June.

Starting the MIDDS GUI

The user accesses the GUI through the MIDDS Toolbar by clicking on the 'FCST Tools' button and choosing 'Lightning Forecast Tool' from the drop-down list (Figure 1). This activates the GUI Tcl/Tk code to determine the date and gather the appropriate data for the equation from MIDDS. The code checks the time and date of the most recent CCAFS sounding (XMR). If it does not match the current day and is not within the time period 0900–1159 UTC, an error message dialog box is displayed (Figure 2). This ensures that data from the previous day and data from sounding times other than 1000 UTC are not used in the equations. The 0900–1159 UTC period allows for the fact that not all 1000 UTC soundings are released precisely at 1000 UTC.

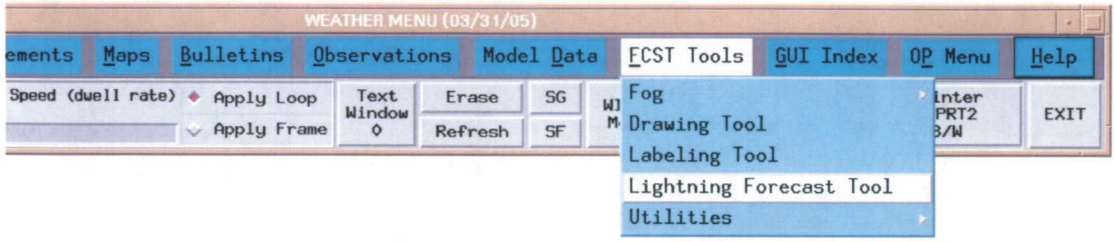

Figure 1. The MIDDS Toolbar showing the 'FCST Tools' button drop-down menu with 'Lightning Forecast Tool' highlighted.

Figure 2 The error message dialog box shown when a 1000 UTC XMR sounding for the current date is not available. The 'OK' button closes the box.

Equation Predictor Dialog Box

Whether or not the 1000 UTC XMR sounding for the current date is available, the equation predictor dialog box is displayed (Figure 3). This will allow the forecasters to use the GUI to create their seven-day forecasts even if data for the current day are not available. The dialog box has five tabs, one for each month. The tab of the current month is displayed initially. The current month, day and sounding time are printed along the top of the dialog box. If the current day's sounding is not available, 'No Current Sounding' will be displayed in place of the date and time in the upper right. The day value can be changed by the up/down arrows or by entering a value manually in the text box. This allows forecasters flexibility when making the seven-day Weekly Planning Forecast. The sounding date and time is formatted by year, day of year, and UTC time. The rest of the dialog box mirrors that of the Excel GUI (Lambert and Wheeler 2005).

Forecasters begin by choosing Yes or No for persistence, then a flow regime. They do not have to enter the sounding parameters as those values are already input by the GUI code and are displayed in their associated text boxes. If there is not a current sounding, the text boxes will be populated with the values from the most recent sounding available. The 'No Current Sounding' message in the top right corner will inform the forecaster that this is the case. If the routines can not find a sounding file of any kind, the text boxes will be populated with the extreme low value in the range of available values for each sounding parameter.

The final step is to click on the 'Calculate Probability' button in the lower right corner of the dialog box. The 'Dismiss' button in the lower left closes the GUI. If the forecaster does not choose a persistence value or flow regime, an error message dialog box similar to that in Figure 2 is displayed telling the forecaster to make a choice. There are separate error message dialog boxes for persistence and flow regime (not shown).

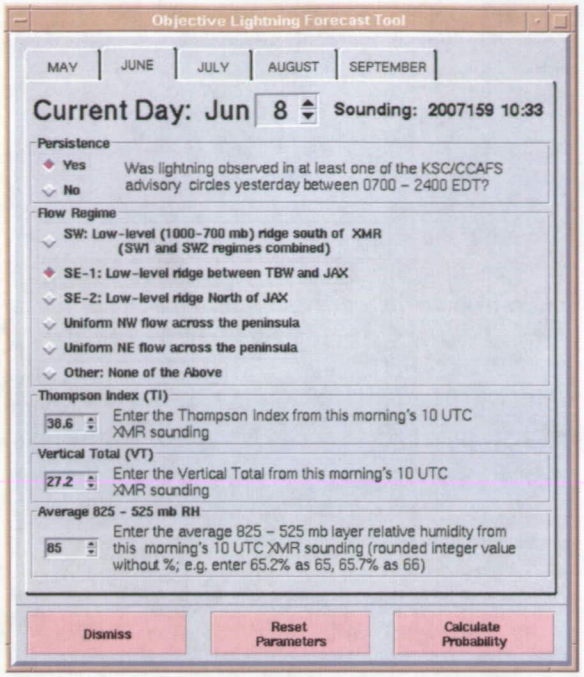

Figure 3. The predictor dialog box for June. A tab for each month is at the top, followed by the date and sounding time, then the predictor values. The 'Dismiss' button closes the GUI, the 'Reset Parameters' button resets the sounding parameters to the original values, and the 'Calculate Probability' button displays the probability output dialog box (Figure 4).

Output Dialog Box

When the user clicks the 'Calculate Probability' button in the equation predictor dialog box, the probability of lightning occurrence for the day is displayed in a dialog box (Figure 4). The GUI code also outputs a file that contains all of the parameter values input by the user to calculate the probability. This file is currently named LtgProb.txt, and resides in the MIDDS data directory.

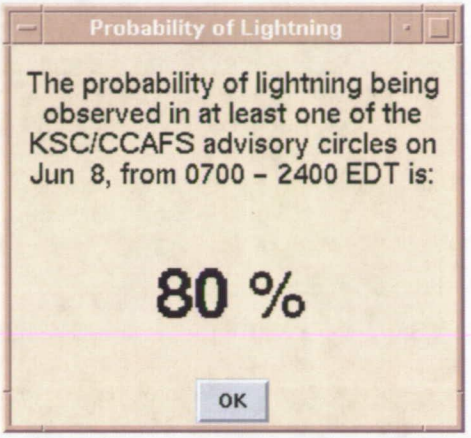

Figure 4. The output dialog box showing the probability of lightning occurrence for the day as calculated by the equation. The 'OK' button closes the box.

Final Report

Ms. Lambert completed a draft of the final report and submitted it for an internal AMU review. It will be distributed to customers in July after she makes modifications to the report from the internal review. Based on the current timeline, Ms. Lambert expects to have NASA approval for final distribution of the report at the end of July or beginning of August.

Contact Ms Lambert at 321-853-8130 or lambert.winnie@ensco.com for more information.

Peak Wind Tool for General Forecasting (Mr. Barrett, Dr. Short, and Ms. Lambert)

The expected peak wind speed for the day is an important element in the daily morning forecast for ground and space launch operations at KSC and CCAFS. The 45 WS must issue forecast advisories for KSC/CCAFS when they expect peak gusts to exceed 35 kt, 50 kt, and 60 kt thresholds at any level from the surface to 300 ft. However, the 45 WS forecasters indicate that peak wind speeds are a challenging parameter to forecast, regardless of their value. They requested that the AMU develop a tool to help them forecast the daily average and highest peak non-convective wind speed, and the timing of the peak speed, from the surface to 300 ft on KSC/CCAFS for the cool season (October-April). The AMU is using a 4-year database of high resolution soundings and other observational data available by the morning weather briefing at 0700 local time to develop a tool that provides a forecast of the peak wind speed for the day, its timing, and the average wind speed at the time of the peak.

Development of Prediction Equations

Mr. Barrett created linear regression equations to predict the highest peak wind speed of the day, the timing of the peak, and the average speed at the time of the peak in the surface–300 ft layer during the cool season. The equations were

developed using KSC/CCAFS wind tower network, XMR, and Shuttle Landing Facility (SLF) hourly surface observations taken during the cool season months from October 2002 to February 2007. Mr. Barrett developed two sets of equations: one for the 11-hour daytime period from 8:00 am to 7:00 pm EST, and the other for the 24-hour period from 8:00 am to 8:00 am EST the following morning. The daily 24-Hour Planning Forecast is issued each morning by the 45 WS for the period from 8:00 am to 8:00 am local time. The equations will give the end user the option of predicting winds for the 11-hour daytime period or for the entire 24-hour day.

Peak Wind Speed Equations

Mr. Barrett created three forecast equations for each time period to predict the daily peak wind speed. He first created a dataset containing data from all days in which the KSC/CCAFS tower network observations and morning XMR soundings were available. The first equation used all days in this dataset. He created the second and third equations from two stratifications of this dataset:

- Four categories depending on whether or not there was a temperature inversion from the surface to 500 ft and whether or not precipitation occurred at or near the SLF, and
- Six synoptic patterns described in the previous AMU Quarterly Report (Q2 FY07).

The inversion/precipitation stratification was used to develop the second equation, and the synoptic pattern stratification was used to develop the third equation. The two stratification methods were not combined together as this would have resulted in 24 categories that contained too few days from which to have drawn a robust statistical relationship. The linear regression equations that minimized the mean absolute error (MAE) and maximized the coefficient of determination (R^2) were selected for the forecast tool. The R^2 is 1 for a perfect correlation between the predictors and predictand and 0 for no correlation.

Mr. Barrett analyzed the following candidate predictors from the morning XMR sounding for the first equation:

- The strongest wind in the lowest 3000, 4000, and 5000 ft;
- The wind speed at the top of the surface-based temperature inversion, or the surface wind speed if no inversion was observed;
- The depth of the surface-based inversion in feet, which was set to zero If no inversion was observed;
- The strength of the surface-based inversion in degrees Celsius, which was also set to zero if no inversion was observed; and
- Persistence, defined as the peak wind speed from the previous day.

He found that the most important predictors for the first equation were the strongest wind in the lowest 3000 ft of the sounding, inversion depth, and inversion strength.

For second and third equations, Mr. Barrett analyzed the following candidate predictors from the morning XMR sounding:

- The strongest wind in the lowest 3000, 4000 and 5000 ft; and
- The wind speed at the top of the surface-based inversion, or the surface wind speed if no inversion was observed.

The best predictor for both of these equations was the strongest wind in the lowest 3000 ft of the sounding. Mr. Barrett used the predictors that were created at the beginning of this task for the second and third equations. Persistence and inversion depth and strength were added later, and the time constraint only allowed them to be tested for the first equation.

Figure 5 andFigure 6 show the skill of the predictors analyzed for the second equation. The predictability of peak wind speeds varied within the days stratified by inversion and precipitation occurrence. The MAE was lowest on days with a surface-based temperature inversion and no precipitation at the SLF. However, R^2 was highest on days with no inversion and no precipitation at the SLF. Overall, the equations showed the least skill occurred on days with precipitation at the SLF. Peak winds appeared to be most predictable on dry and stable days. The figures also show that the predictive skill for the 11-hour period is greater than that for the 24-hour period. Mr. Barrett investigated whether all of the equations for the 11-hour daytime period were more accurate than the equations for the 24-hour period. As was seen in the figures, he found the 11-hour equations to be more skillful than the 24-hour equations for all three stratifications.

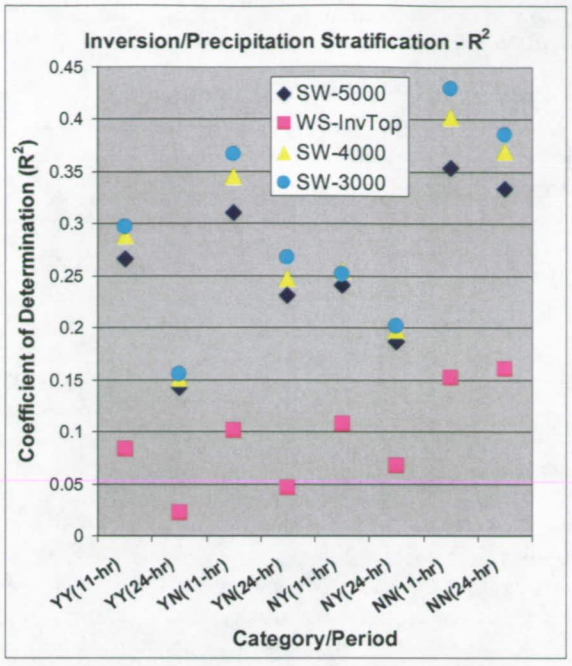

Figure 5. The R^2 values for several predictors using the inversion/precipitation stratification. SW-5000 is the strongest wind in the lowest 5000 ft, WS-InvTop is the wind speed at the top of the inversion, SW-4000 is the strongest wind in the lowest 4000 ft and SW-3000 is the strongest wind in the lowest 3000 ft. On the x-axis, YY is days with both an inversion and precipitation, YN is days with an inversion but no precipitation, NY is days with no inversion and precipitation, and NN is days with no inversion and no precipitation.

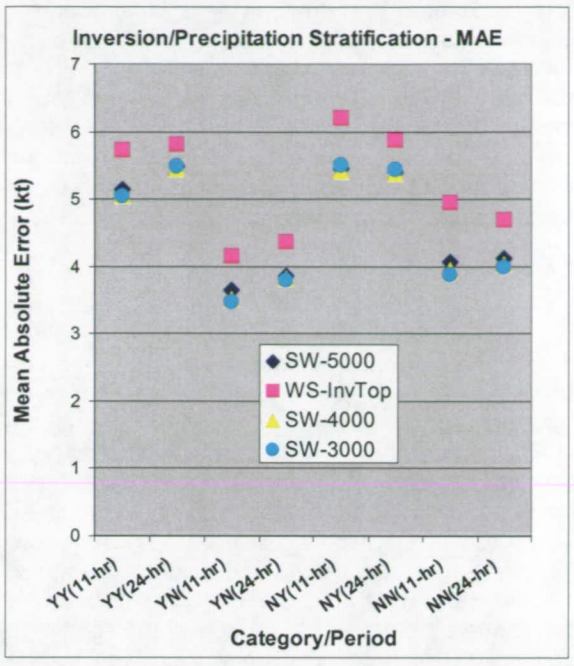

Figure 6. The MAE values for several predictors using the inversion/precipitation stratification. SW-5000 is the strongest wind in the lowest 5000 ft, WS-InvTop is the wind speed at the top of the inversion, SW-4000 is the strongest wind in the lowest 4000 ft and SW-3000 is the strongest wind in the lowest 3000 ft. On the x-axis, YY is days with both an inversion and precipitation, YN is days with an inversion but no precipitation, NY is days with no inversion and precipitation, and NN is days with no inversion and no precipitation.

The predictability of the peak wind speed varied with the synoptic weather pattern (not shown). The least skill in predicting peak wind speeds occurred with an approaching front, while the best skill occurred with easterly winds and high pressure to the north of Florida. One possible explanation could be that easterly winds indicate a slowly changing wind pattern, while a front indicates a more dynamic wind pattern.

The value for forecast peak wind speed was created using an ensemble of all three equations, since all of them showed skill above persistence. The peak wind speeds from the three equations were weighted by the inverse of the MAE, then averaged.

Peak Wind Speed Timing Equations

Mr. Barrett created three equations for each time period to predict the timing of the peak wind speed. The first equation was developed using all days in the period. It is a multiple linear regression with inversion depth and inversion strength as predictors. The peak wind tended to occur slightly later when the inversion was strong and deep.

He developed the second equation using the data stratified by synoptic pattern. The peak wind tended to occur the earliest when there was either a front to the south of Florida, or westerly winds with high pressure to the south or west of Florida. The peak wind tended to occur the latest when there was either a front approaching Florida from the north, or variable winds with high pressure across Florida. Further investigation is necessary to provide an explanation.

He developed the third equation using the inversion/precipitation stratification, which showed the best skill out of the three. The daytime peak wind occurred earliest on days with no inversion

or precipitation. The daytime peak wind occurred latest on days with precipitation and an inversion. An inversion tends to delay the peak wind until surface heating or temperature advection allows the inversion to break. Mr. Barrett investigated the relationship between the peak wind speed and the timing of the peak wind; however, this predictor exhibited less skill than the others.

Average Wind Speed Equations

Mr. Barrett created one equation for each time period to predict the 5-minute average wind speed at the time of the maximum peak wind speed. The linear regression equation used the observed maximum peak speed as the predictor and the average speed at the same time as the predictand. For operations, the equation to predict the average wind speed will use the weighted average value calculated from the peak speed forecast from the three equations discussed earlier. He investigated the relationship between the observed peak wind speed and the gust ratio of peak to average wind speed, as well as the relationship between the height of the sensor reporting the peak wind and the gust ratio. However, these predictors showed little skill in forecasting the average wind speed.

Development of Forecast Tool

Mr. Barrett developed an Excel GUI to display the predicted peak speed and timing from the three equations for each, and the associated average speed. It displayed the values from all three equations, showing the user the range of possible peak wind speeds.

After creating a prototype GUI, Mr. Barrett collaborated with Mr. McNamara and Mr. Roeder of the 45 WS on design changes that would make the GUI useful in operations. In the first version of the forecast tool, the predicted winds were displayed for both the 11- and 24-hour periods. The 45 WS reviewed the GUI and requested that the three values for the timing and speed of the peak wind speed be combined into one. They also requested that the tool include the probability of the peak wind speed exceeding 34 kt, 49 kt, and 59 kt. Mr. Barrett is currently updating the tool based on these requests.

Contact Mr. Barrett at 321-853-8205 or barrett.joe@ensco.com, for more information.

Situational Lightning Climatologies for Central Florida, Phase II (Dr. Bauman)

The threat of lightning is a daily concern during the warm season in Florida. Recent research has revealed distinct spatial and temporal distributions of lightning occurrence that are strongly influenced by large-scale atmospheric flow regimes. In Phase I, Ms. Lambert created 6- and 24-hour gridded CG lightning density and frequency climatologies based on the flow regime that the forecasters at the National Weather Service in Melbourne, FL (NWS MLB) use to issue daily lightning threat maps for their county warning area (Lambert et al. 2006). Phase II of this work consisted of three parts. In the first part, Dr. Short created climatological soundings of wind speed, wind direction, temperature, and dew point at Jacksonville, Tampa, Miami, and XMR for each of eight flow regimes from a 16-year database of soundings (Short 2006). In the second part of the Phase II work, Dr. Bauman calculated the same climatologies as in Phase I for the two 12-hour periods 0000–1200 UTC and 1200–2400 UTC. In the third part of the Phase II work, Dr. Bauman created the flow regime climatologies for 5-, 10-, 20-, and 30-n mi circles centered on the SLF in 1-, 3-, and 6-hour increments. The 5- and 10-n mi circles are consistent with the aviation forecast requirements at NWS MLB. The 20- and 30-n mi circles at the SLF will assist SMG in making forecasts for FR violations of lightning occurrence during a shuttle landing.

SLF and Other Airport Climatologies

Originally, the code from this task was to be delivered to NWS MLB so they could create the climatologies for the other seven airports at which they have aviation forecast responsibilities: Daytona Beach (DAB), Sanford (SFB), Leesburg (LEE), Orlando (MCO), Kissimmee (ISM), Melbourne (MLB) and Vero Beach (VRB). However, once Dr. Bauman set up the code for the SLF, he found it relatively easy to modify and run it for these airports, including St. Lucie (FPR), which the NWS MLB asked the AMU to include if time permitted. The locations of the sites for which the climatologies were created are shown in Figure 7 with their 5-, 10-, 20-, and 30-n mi circles.

Dr. Bauman modified the Phase I code to determine the indices of the grid boxes comprising the requested circles centered on the SLF and the other airports. The modified code produced results that created one value for the total number of lightning strikes in each circle based on the sum of the number of lightning strikes in all the

boxes within the area of each circle. The climatology calculations in the code remained the same. Instead of a value for each grid box as in Lambert et al. (2006), one value each for the probability of lightning occurrence and the mean number of strikes per flow regime was created for each circle. The resulting values included 1-, 3- and 6-hour climatologies in the 5-, 10-, 20- and 30 n mi circles for each of eight Florida flow regimes (Lericos et al. 2002; Lambert and Wheeler 2005).

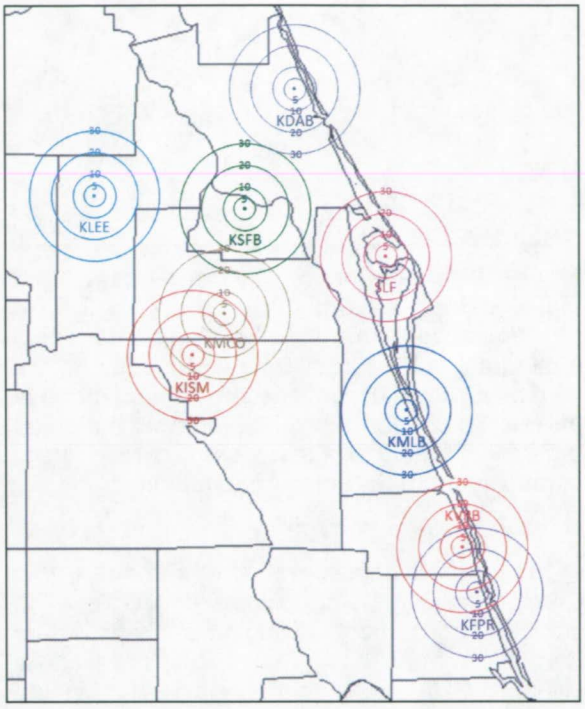

Figure 7. Map of east-central Florida showing locations of the SLF and eight airports. The circles around each location indicate the distance from the center of each site from 5 to 30 n mi.

Modifying Existing FOTRAN Code

The bulk of the work for Dr. Bauman in this task involved modifying the existing FORTRAN code from Phase I to produce the climatological lightning probabilities during the specified time intervals and circles at each site. It required careful rewriting of pieces of the code to produce a single probability for each circle and time interval. Once the code was modified, Dr. Bauman tested it on the SLF circles to make sure the conversion from the 405 x 377 grid domain (Figure 8) containing the lightning data in 2.5 x 2.5 km grid boxes to the latitude/longitude (lat/lon) of the SLF was working properly. After determining the location of the SLF within the grid domain, Dr. Bauman modified the code and imported the output into ArcGIS software and plotted the grid over a map with the SLF. This map is shown in Figure 9. The domain approximating a 30 n mi circle from the center of the SLF is 22 x 22 grid boxes. As Figure 9 shows, within the 22 x 22 grid boxes, the nearest grid square to the center of the SLF runway at 28.6150N, 80.6945W is (284,205). Dr. Bauman carried out the same procedure for the other eight airports to verify the grid domain was properly placed relative to the lat/lon of each location before calculating the probabilities.

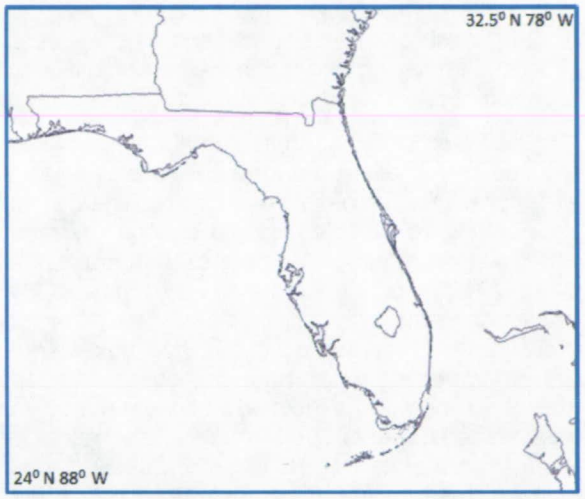

Figure 8. Domain of 405 x 377 2.5 x 2.5 km grid boxes of lightning data.

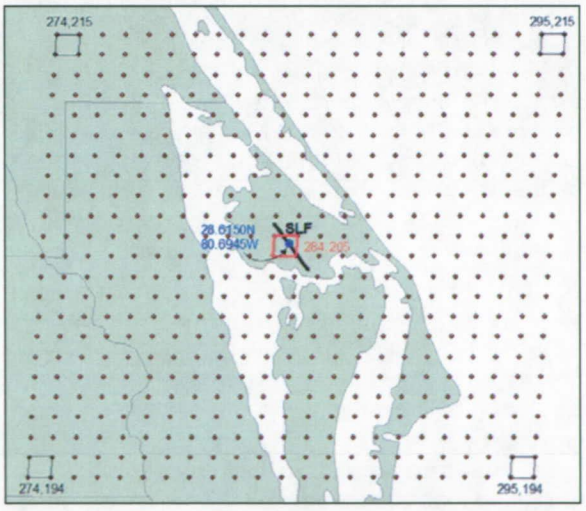

Figure 9. The 30 n mi grid with the SLF runway at the center. The four corners of the grid show the grid square coordinates (x, y). The red square is the grid box nearest the centers of the 30 n mi grid and SLF. The blue dot is at the lat/lon of the SLF runway center.

Approximating Circles with a Square Grid

The CG lightning data were provided as the number of strikes per hour in 2.5 x 2.5 km grid boxes, and the center point of each runway was not always in the center of or at an apex of a grid box. Because the data were in the form of grid boxes, each of the circles was approximated by a square area around each circle comprised of the grid boxes. Figure 10 shows the size of the four circles used in this work overlaid on a grid of 2.5 x 2.5 km grid boxes. This figure represents an idealized case where the center of a runway is at the middle of the range rings. This was not the case for each of the nine locations as they were all offset somewhat from the center of the grid square closest to the center of the circle.

Using squares to approximate the circles resulted in a smaller area for the 5 n mi circle and larger areas for the other three circles. The 5 n mi circle in Figure 10 (blue) is represented by nine grid boxes (blue square). The area of the circle is 67 km^2. The area of the square is 56.25 km^2, 16% smaller than the area of the circle. The 10 n mi circle (red) is represented by 49 grid boxes (red square) about its center. Four grid boxes (shaded red) at the corners are outside of the circle. The area of the square is 306 km^2. This is about 12% larger than the area of the circle at 269 km^2. The 20 n mi circle (green) is represented by 225 grid boxes (green square). There are 48 grid boxes (shaded green) outside of the circle at the four corners of the green square. The area of the circle is 1078 km^2. The area of the square is 1406 km^2, or 23% larger than the area of the circle. Finally, the 30 n mi circle (purple) is represented by 529 grid boxes (purple square). There are 144 grid boxes (shaded purple) outside the circle. The area of the circle is 2425 km^2 and the area of the square is 3306 km^2, or 27% larger than the area of the circle.

The difference in areas between the circles and squares resulted in an underestimate of lightning probabilities for the 5 n mi circle and overestimates for the 10, 20, and 30 n mi circles. To better approximate the probabilities in the circles, Dr. Bauman computed the ratio of the area of each square-circle pair, and then multiplied the associated probabilities by this ratio. Normalizing the ratios in this manner minimized the error of approximating each circle by a square. A more accurate way to create these values would be to use raw lightning data that contain the lat/lon of each strike. Data in that form were not available for this work.

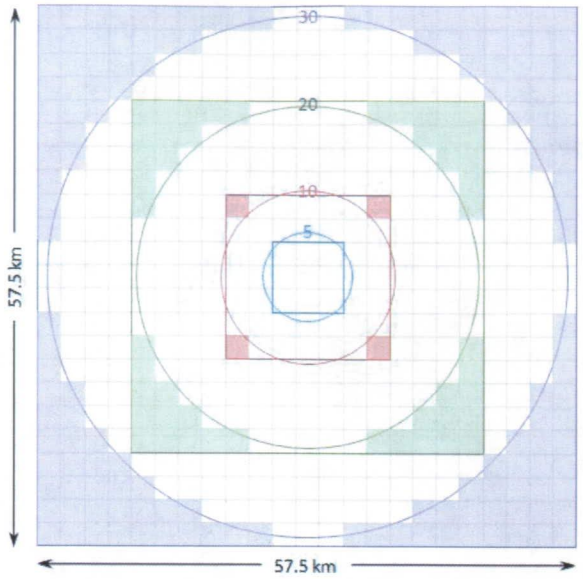

Figure 10. Depiction of the four circles and their idealized relationship to the 2.5 x 2.5 km grid boxes containing the lightning data. The 5 n mi circle is blue, the 10 n mi circle is red, the 20 n mi circle is green, and the 30 n mi circle is purple. The shaded grid boxes show the areas outside of the circles that were included in the computation of lightning probabilities.

Graphical User Interface

The output from the code was imported into Excel spreadsheets to create data tables and graphics for incorporation into a GUI that could be used operationally. Dr. Bauman provided a sample GUI written in Hypertext Markup Language (HTML) to the AMU customers, who liked the format. An HTML GUI is portable among different computer systems and intuitive to use in its similarity to a web browser.

The main page of the GUI (Figure 11) is the starting point. From the navigation menu at the top of the page, forecasters can view the **Data and Definitions** page, which contains helpful information regarding the data, methodology and flow regime definitions, or they can click on a specific site in the navigation menu or the map. Once they have chosen a site, the main page for that site is shown, as for the SLF in Figure 12. The forecasters are presented with two sub-menus on the site page allowing them to view the lightning probabilities based on time interval (1-, 3- or 6-hours) or by flow regime. The main navigation menu remains visible so they can easily switch to another site or access the **Data and Definitions** page.

An example of a time interval page is shown in Figure 13. These are the 3-hour climatologies for all eight flow regimes in all four circles centered on the SLF. The values are in a table on the left side of the page with a corresponding graph to the right of the table. The table/graph combinations represent the climatological values for each of the flow regimes. The 1- and 6-hour pages (not shown) have the same format.

An example of the flow regime page is shown in Figure 14. These are the Southwest-2 flow regime climatologies for all three time intervals in all four circles centered on the SLF. As in the time interval pages, there is a table on the left side of the page with a corresponding line graph to the right of the table. Data for all three time intervals for one flow regime is shown on this page.

Dr. Bauman delivered the final version of the GUI to the AMU customers and began writing the final report. Contact Dr. Bauman at 321-853-8202 or bauman.bill@ensco.com for more information.

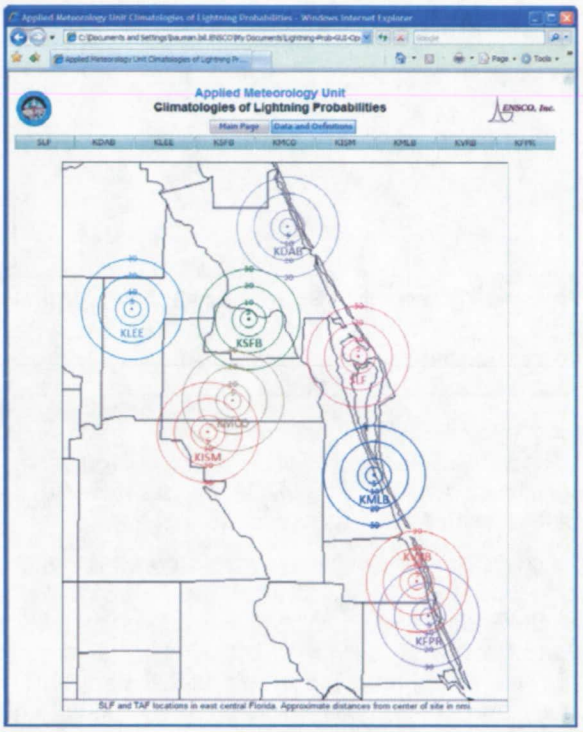

Figure 11. The main page of the GUI provides access to help information and a link to each site via a main navigation menu shown above the map or by clicking on the site on the map.

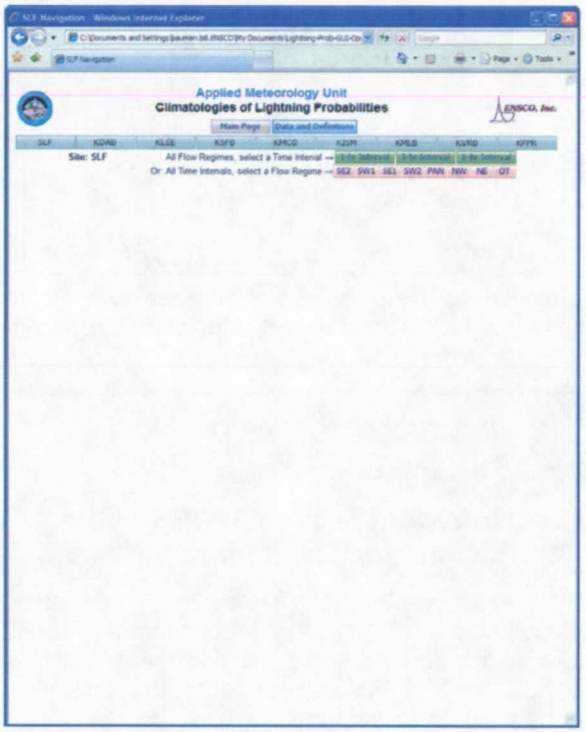

Figure 12. The main page for the SLF site. The two sub-menus allow the forecaster to view the data by time interval or flow regime.

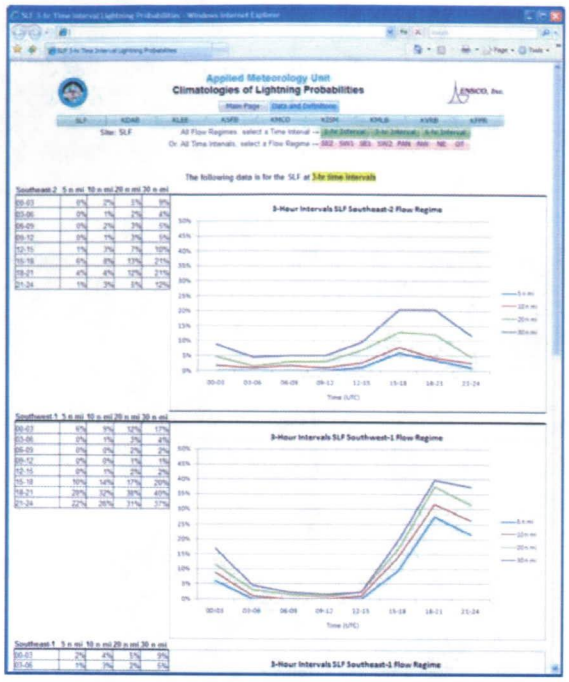

Figure 13. The SLF 3-hour interval data page. Tabular data is on the left with corresponding graphs to the right.

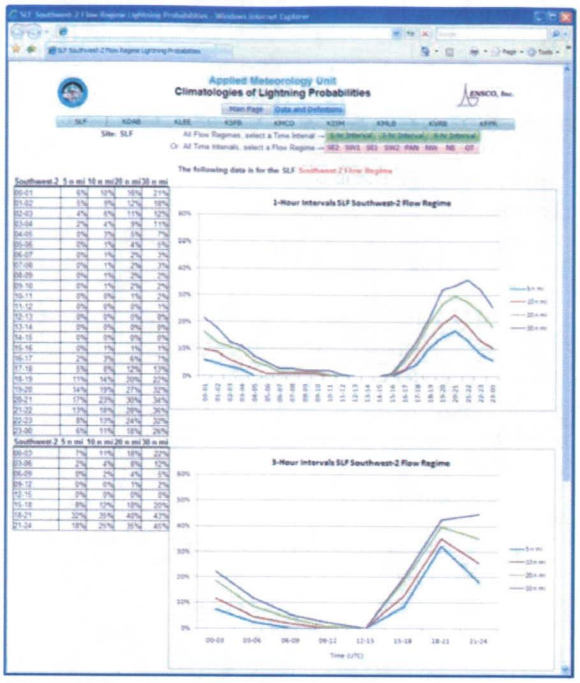

Figure 14. The SLF Southwest-2 flow regime data page. Tabular data is on the left with corresponding graphs to the right.

INSTRUMENTATION AND MEASUREMENT

Anvil Forecast Tool in AWIPS (Mr. Barrett, and Dr. Bauman)

The forecasters at SMG and 45 WS have identified anvil forecasting as one of their most challenging tasks when predicting the probability of LCC or FR violations due to the threat of natural or triggered lightning. In response, the AMU developed an anvil threat corridor graphic that can be overlaid on satellite imagery using the MIDDS. This tool helps forecasters estimate locations where thunderstorms might produce an anvil threat 1, 2, and 3 hours into the future. It has been used extensively in launch and landing operations. The SMG is depending more on the Advanced Weather Interactive Processing System (AWIPS) during operations and the 45 WS may replace their MIDDS with AWIPS. To ensure it will remain available for operations, the forecasters tasked the AMU to transition the anvil tool from MIDDS to AWIPS. The AMU will also create a GUI to ensure easy access to the tool.

Mr. Barrett delivered the software and installation instructions for the Anvil Forecast Tool to SMG and the 45 WS. Dr. Bauman and Mr. Barrett completed the User's Guide (Bauman 2007) and final report (Barrett and Bauman 2007) after addressing comments made during an internal AMU and external customer review. After receiving final approval from NASA, the two reports were distributed to the customers and posted on the AMU website at the URL http://science.ksc.nasa.gov/amu/final.html.

Contact Mr. Barrett at 321-853-8205 or barrett.joe@ensco.com, or Dr. Bauman at 321-853-8202 or bauman.bill@ensco.com for more information on this task.

Volume Averaged Height Integrated Radar Reflectivity (VAHIRR) Algorithm (Mr. Barrett, Ms. Miller, Ms. Charnasky, Dr. Merceret, and Mr. Gillen)

Lightning LCC (LLCC) are used for all launches, whether Government or commercial, using a Government or civilian range (Willett et al. 1999). Shuttle lightning FR are also used for all landings. These rules are designed to avoid natural and triggered lightning strikes to space vehicles, which can endanger the vehicle, payload, and general public. The current LLCC for anvil clouds, meant to avoid triggered lightning, have been shown to be overly restrictive. They ensure safety, but falsely warn of danger and lead to costly launch delays and scrubs. A new LLCC for anvil clouds, and an associated radar algorithm needed to evaluate that new LLCC, were developed using data collected by the Airborne Field Mill research program managed by KSC (Dye et al. 2006, 2007). Dr. Harry Koons of Aerospace Corporation conducted a risk analysis of the VAHIRR algorithm. The results indicated that the LLCC based on the VAHIRR algorithm would pose a negligible risk of flying through hazardous electric fields.

In the previous Quarter (AMU Quarterly Report Q2 FY07), the AMU determined that additional software development and testing of the VAHIRR radar product was necessary in order to address the radar cone of silence, how the cloud thickness is calculated, and the elevation of the radar when calculating the height and thickness of clouds. Ms. Miller implemented the necessary software changes.

Mr. Barrett wrote a Tcl script that will archive radar products on the Open Radar Product Generator (ORPG) clone in real-time. Each time a volume scan of the radar is completed, the VAHIRR product will be generated and stored in the product database. The product database is one large file that stores all radar products generated by the ORPG-clone, not just the VAHIRR product. When the product database reaches a predetermined maximum size, the oldest products are purged to make room for newly generated products. The main purpose of the script is to archive VAHIRR products to prevent them from being purged. The script can also be used to store VAHIRR products as individual files so they can be viewed in AWIPS.

Mr. Barrett and Ms. Charnasky installed an additional ORPG-clone running Build 8 of the ORPG software at the ENSCO Cocoa Beach (CB) office. This machine will be used to carry out testing of the VAHIRR radar product. The testing tools were not compatible with the existing CB office's ORPG-clone that is running Build 6 of the ORPG software. Ms. Charnasky and Ms. Miller used the testing tools to create two tailored volume scans of level II radar data. One of the tailored volume scans is the radar baseline dataset. In this volume scan, reflectivity values are assigned to specific azimuth and one or more of nine radar elevations as shown in Figure 15:

- For the 11 sectors between 0 and 180 degrees azimuth, the values shown in Figure 15 are at radar elevation 4. For elevations 1–3 and 5–9, the value is -10 dBZ.
- Between 180.1 and 225.0 degrees azimuth, the value 0.5 dBZ is at radar elevations 8–9. For elevations 1-7, the value is -10 dBZ.
- Between 225.1 and 270.0 degrees azimuth, the value 0.5 dBZ is at radar elevations 1–9.
- Between 270.1 and 315.0 degrees azimuth, the value 0.5 dBZ is at radar elevation 1 and 10 dBZ is at radar elevations 2–3. For elevations 4–9, the value is -10 dBZ.
- Between 315.1 and 359.9 degrees azimuth, the value 0.5 dBZ is at radar elevation 1. For elevations 2–9, the value is -10 dBZ.

The other tailored volume scan is used in the reflectivity average for the multiple elevation angles test procedure.

Ms. Charnasky and Mr. Barrett updated the test plan and procedures to create a comprehensive test the VAHIRR parameters. Dr. Merceret is currently reviewing the test plan and procedures. The tests include:

- A baseline test in which the VAHIRR product is generated from the radar baseline dataset. The product output must be the same as a pre-computed VAHIRR product shown in Figure 16.
- A freezing level test that demonstrates whether the VAHIRR product produces the correct results when varying the height of the freezing level.

- Cone-of-silence test that demonstrates whether the VAHIRR product produces the correct results when varying the cone of silence height.
- Reflectivity average for multiple elevation angles test that demonstrates whether the VAHIRR product averages all elevation scans for points with reflectivity greater than or equal to 0 dBZ. This verifies that the product does not stop calculating a VAHIRR value when negative reflectivity is encountered and verifies whether the product produces the correct results when varying cloud thickness in relation to the height of the freezing level.
- ABFM comparison test that compares ENSCO's implementation of the VAHIRR algorithm to the implementation by the Airborne Field Mill II Project (Dye et al. 2004).

For more information, contact Ms. Miller at 321-783-9735 ext. 221 or miller.juli@ensco.com; Mr. Barrett at barrett.joe@ensco.com or 321-853-8205, or Dr. Merceret at 321-867-0818 or Francis.J.Merceret@nasa.gov.

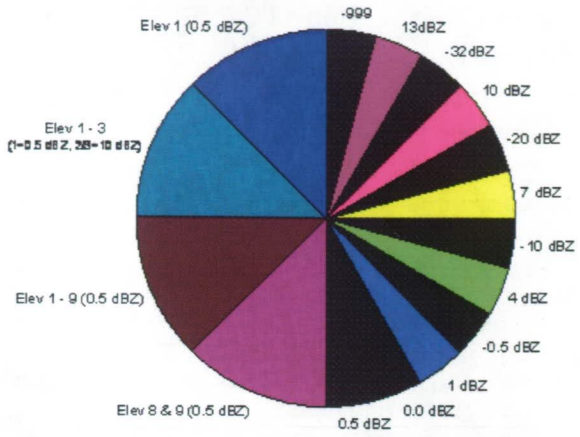

Figure 15. The baseline dataset used in the baseline, freezing level, and cone-of-silence tests. Between 0 (top) and 180 (bottom) degrees clockwise, the figure shows the reflectivity values (in dBZ) at radar elevation 4. Between 180 and 360 degrees, the figure shows the radar elevations and associated reflectivity values. For radar elevations not shown, -10 dBZ is assigned.

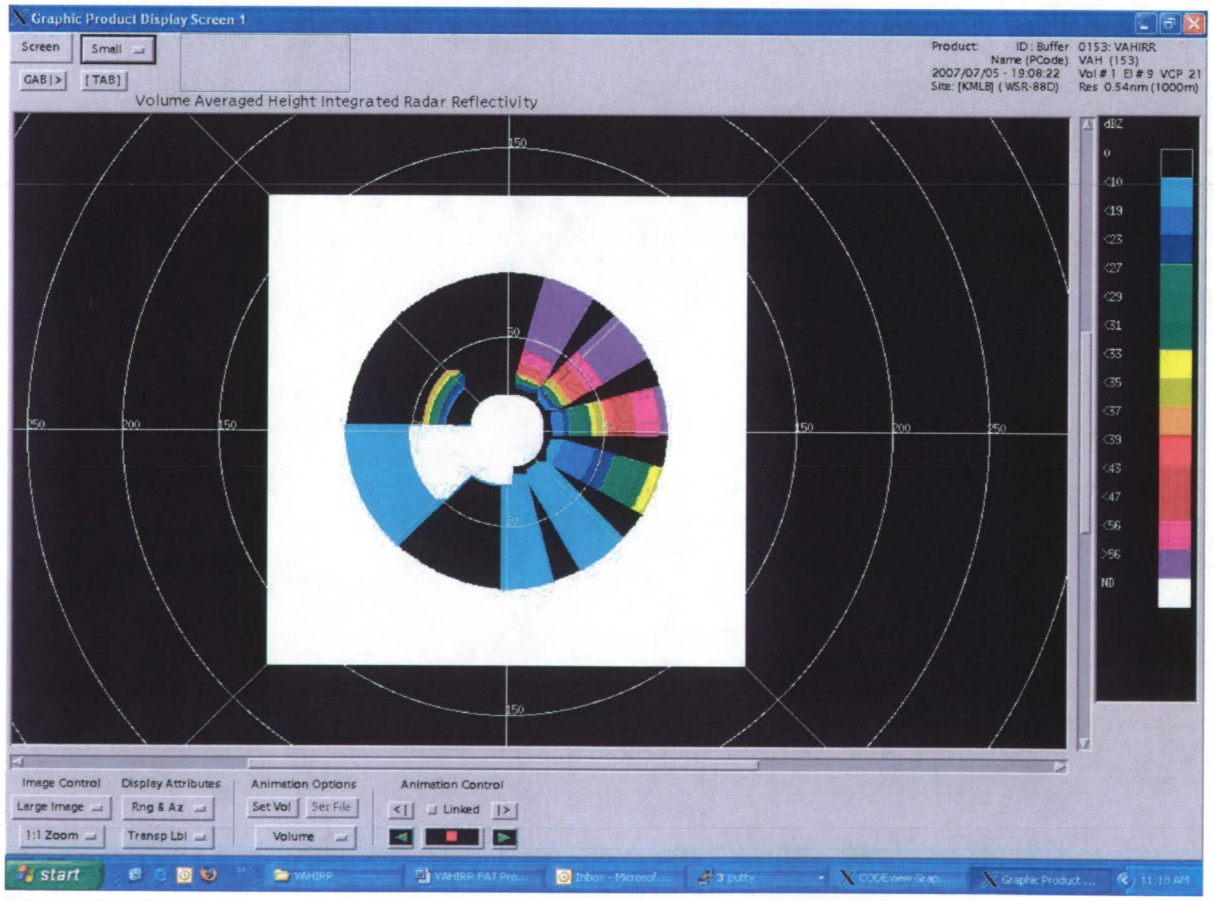

Figure 16. The output VAHIRR product using the baseline dataset shown in Figure 15.

Tower Data Skew-T Tool (Mr. Wheeler)

The rapid reduction in visibility and ceiling associated with marine-layer incursions is a concern to 30th Weather Squadron (30 WS) forecasters during launch operations at Vandenberg Air Force Base (VAFB). Such conditions will become a launch safety concern with new launch vehicles that require they be viewable by remote cameras until radar lock-on. The incursion occurs when the marine layer (cooler/moist air) moves inland from the Pacific Ocean. The VAFB radiosonde is a critical data source in analyzing this phenomenon. To fill in for a temporary loss of radiosonde data due to software or sonde problems, the 30 WS developed the Tower Data Skew-T Tool (Wells 2005) to help monitor the progress of marine-layer incursions. The AMU will evaluate the effectiveness of this tool for the 30 WS using data collected during two previous marine-layer incursion events.

Marine-layer incursions tend to occur during the summer months when California is influenced by a sub-tropical high over the eastern Pacific with a heat induced thermal trough up through the central California interior. This produces a predominant northwest flow across the California coast. At times, this regime is replaced by a southerly surge that causes near-surface cooling and the development of stratus clouds along the coast of California (Felsch 1993).

Mr. Schmeiser of the 30 WS provided the data needed for the study from eight wind towers and the VAFB soundings for August 2006. Figure 17 is a map of the instrument locations on VAFB with the eight wind tower and sounding locations indicated by red triangles and a circle, respectively. The tower data include temperature and humidity at 6 and 54 ft, and wind direction and speed at 12 and 54 ft.

The Skew-T tool is an Excel application that allows the forecaster to input temperature and relative humidity values from the eight wind towers and the VAFB Automatic Surface Observing System (ASOS) observation. These observations are merged to develop a composite vertical profile of the lower atmosphere up to 2200 ft above mean sea level (MSL) meant to approximate the VAFB sounding when that data source is not available. The tool can plot up to four profiles at one hour intervals, allowing the user to monitor and compare temperature and moisture changes in the lower atmosphere for up to four hours.

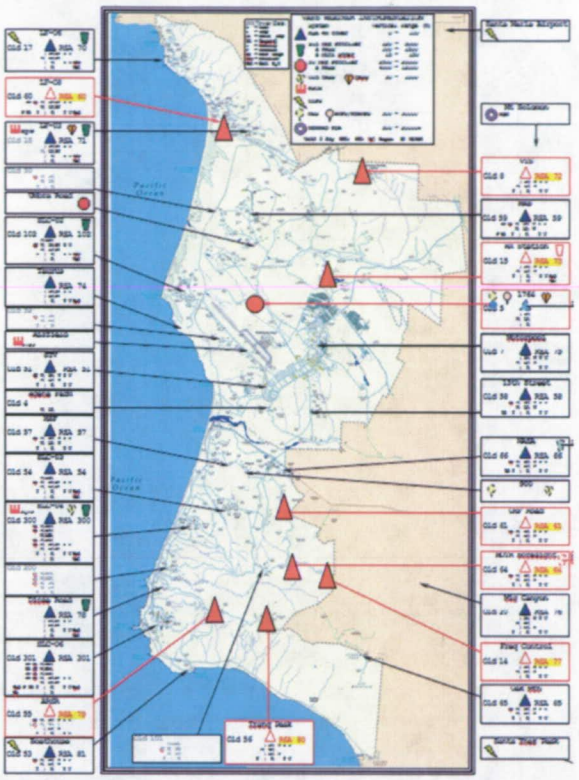

Figure 17. Map of VAFB showing the locations of the eight towers (red triangles) and the sounding (red circle).

An example of the Skew-T Tool is shown in Figure 18. A description of how to use the tool is in the blue box at the bottom left. The table on the left is where the user enters the temperature and relative humidity (RH) value for each tower and ASOS observation, which are the data from which the composite profile is built. There are four areas in this table, one for each hour with the most recent set of observations at the top. As the user enters values the program plots the temperature and dew point temperature profiles.

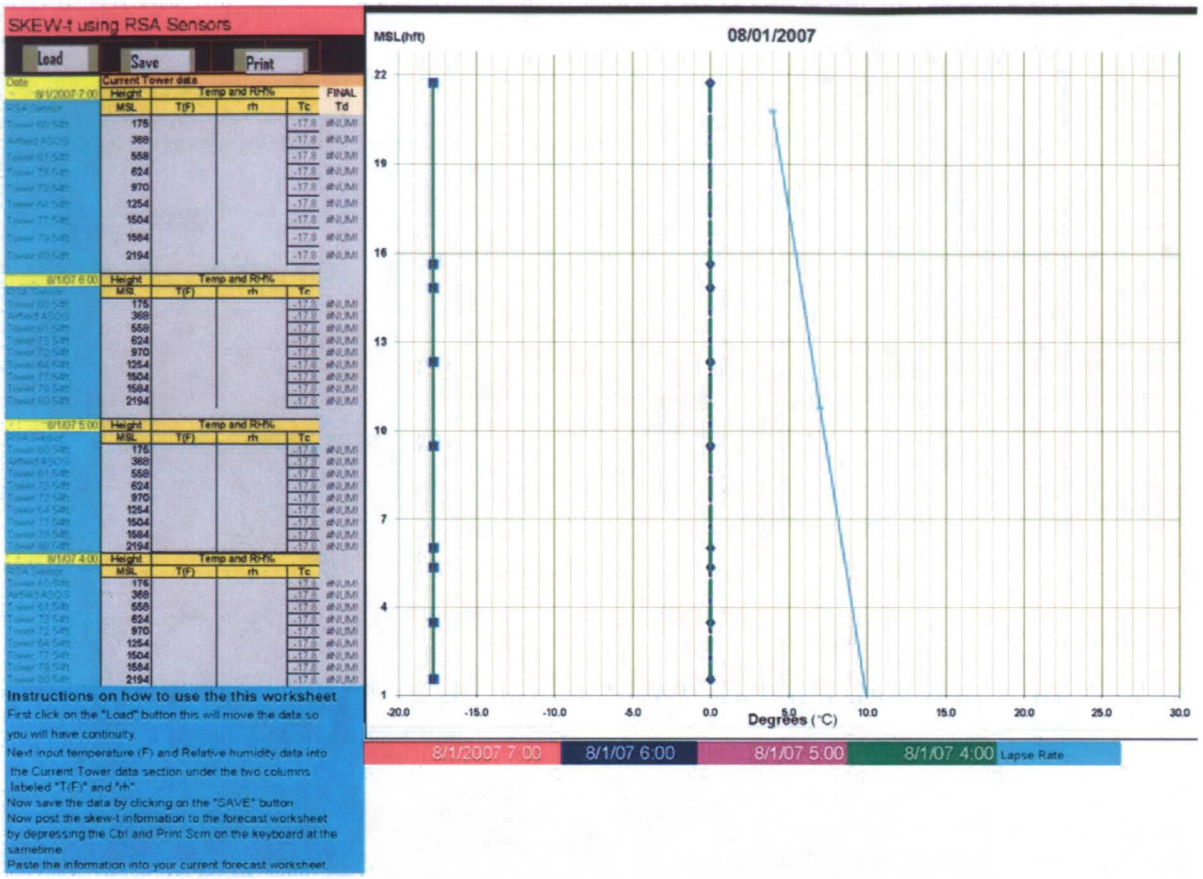

Figure 18. The Skew-T tool with no data entered. The four areas in the table on the left are for the temperature and RH data from the tower and ASOS observations for four hours, most recent hour at the top. The graph in the right displays the profiles created from the data in the tables with height in hundreds of feet on the vertical axis and temperature in C along the horizontal axis. The diagonal cyan line represents the standard atmospheric lapse rate. The colors at the bottom show what color the profile for each time would be: green (oldest), purple, blue, and red (most recent).

Mr. Wheeler processed the rawinsonde data valid at 0000 and 1200 UTC and 1-minute tower data collected during 1–25 August 2006. He converted the datasets from the Range Standardization and Automation (RSA) format into comma delimited format and then imported them into Excel. Because of missing data, the period of record was reduced to 10–21 August 2006.

10-11 August 2006 Case Study

By 0000 UTC 11 August, the VAFB area was experiencing a typical summer weather pattern dominated by an east Pacific high, a surface low in southern California and a heat induced thermal trough up into central California (Figure 19). This pattern develops a northwest surface wind from the Pacific Ocean toward the California coast.

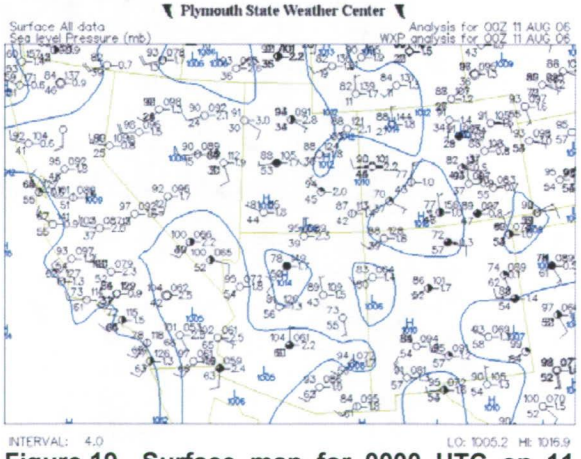

Figure 19. Surface map for 0000 UTC on 11 August 2006.

Figure 20 shows the VAFB rawinsonde and Skew-T composite profiles of temperature and dew point observations at 2300 UTC on 10 August, the release time for the 0000 UTC 11 August VAFB sounding. The temperature profile from the towers shows a cooler surface temperature compared the sounding. The first tower representing the lowest height in the composite sounding is near the Pacific Ocean where the surface temperature is generally cooler. Inland towers are used for the other heights above the surface where it tends to be warmer and dryer. The example in Figure 20 shows the composite profile to be generally warmer and dryer aloft than the sounding in the vertical. There are several reasons for this:

- The VAFB rawinsonde is released at a single point, where the tower generated Skew-T is from several sensors over a large area;
- Each wind tower sensor is at a different elevation and the Skew-T tool builds a composite sounding using data that is closest to 0 ft MSL (near the coast) to approximately 2200 ft MSL (furthest inland); and
- Due to the changing elevations and wind flow patterns, upslope and down-slope conditions will modify the tower composite sounding.

Not until after sunset when the lower atmosphere stabilizes and becomes more homogeneous with light winds could the sounding and tower composite profiles be more similar.

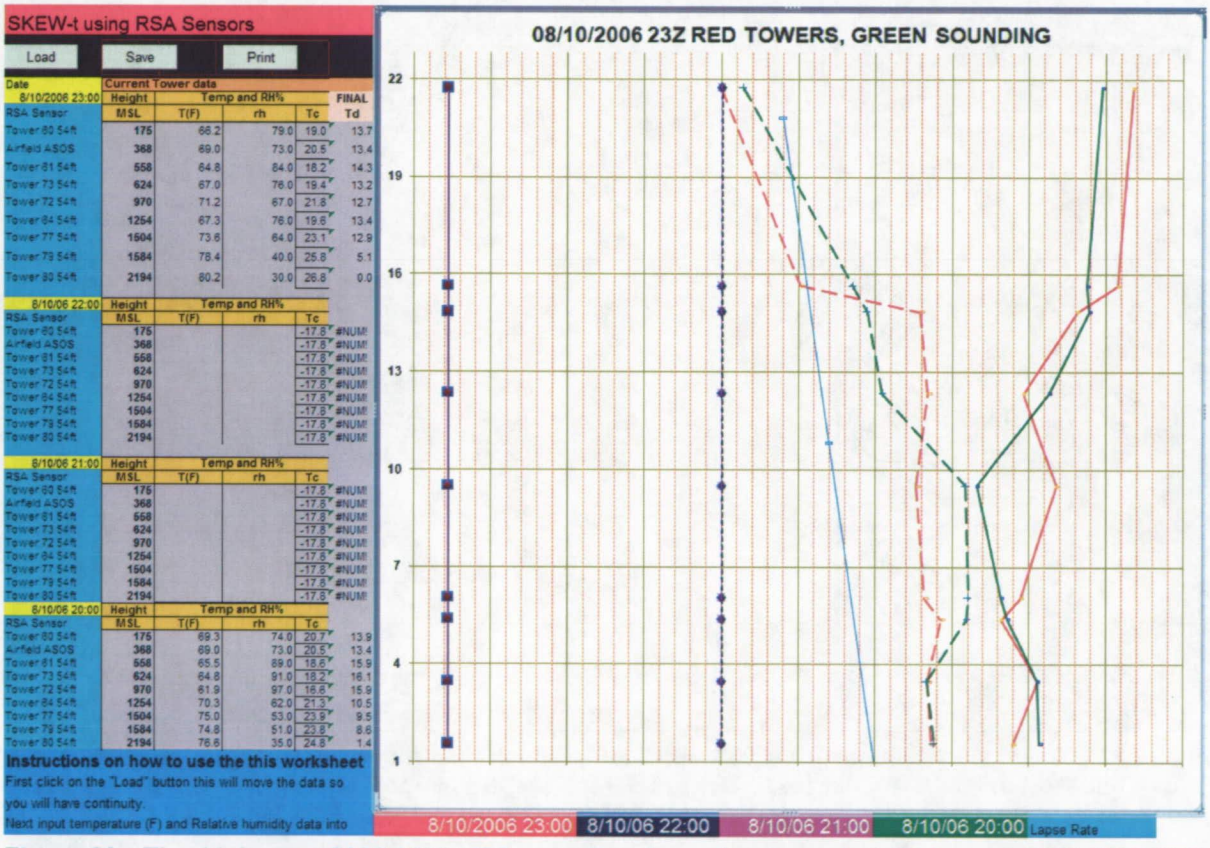

Figure 20. The 11 August 2006 0000 UTC sounding (green), released at 10 August 2006 2300 UTC and the Skew-T Tower plot at 2300 UTC. The solid lines represent the temperature profiles and the dashed lines represent the dew point temperature profiles.

Analysis Summary

Due to afternoon surface heating and terrain effects on the sensors such as upslope and downslope winds, the Skew-T tool is not effective as an afternoon rawinsonde replacement tool. The Skew-T tool is most useful during the late evening/early morning hours when the lower atmosphere has stabilized and the winds are light (less than 5 kt). Under these conditions, the tool allows the forecasters to monitor the conditions of the lower atmosphere to determine if there is increasing or decreasing moisture, to determine if fog and stratus will develop if not already there or to determine approximately when the conditions may break. Figure 21 is a four-hour trend plot of the conditions that occurred on 10 August beginning at 2300 UTC (green) going to 11 August at 0200 UTC (red) when a stratus ceiling at 200 ft occurred. Note the trend of increasing moisture to almost saturation in the low levels by 0200 UTC.

Contact Mr. Wheeler at 321-853-8105 or wheeler.mark@ensco.com more information.

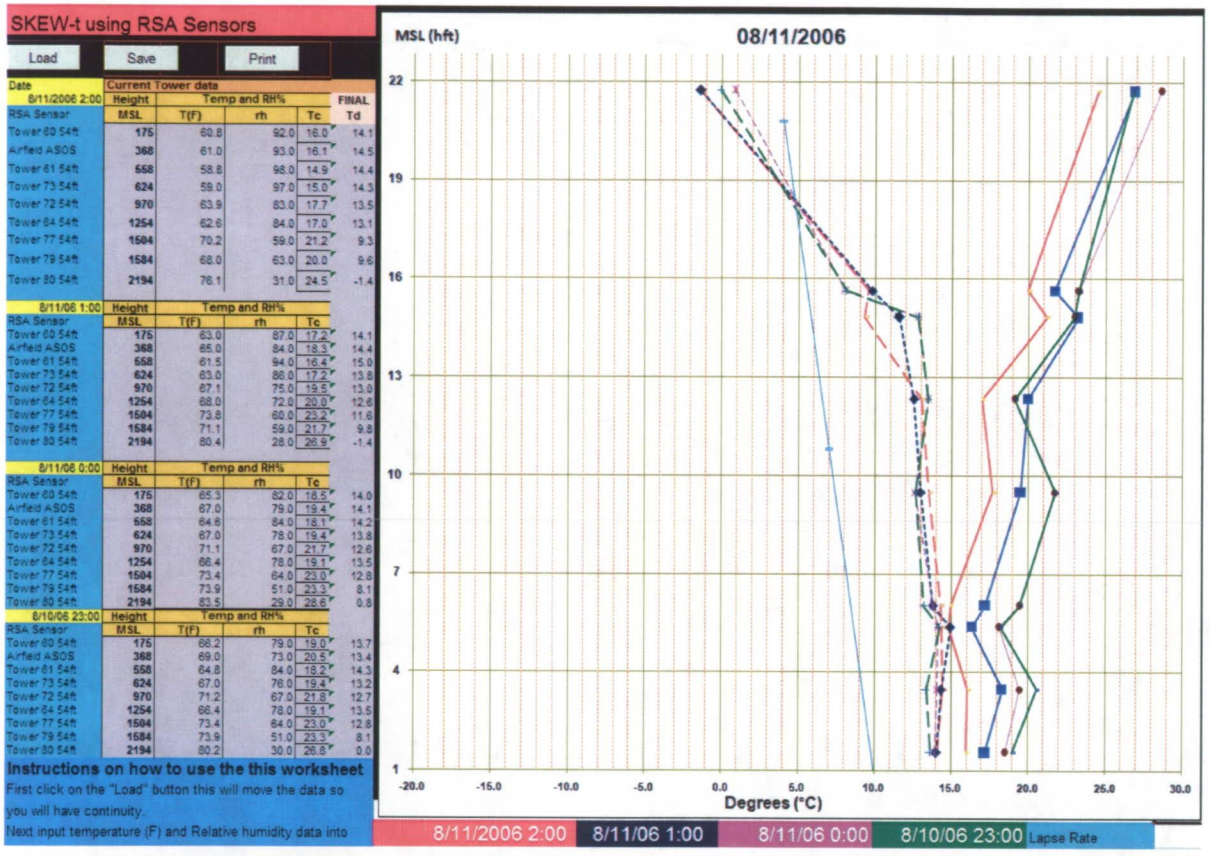

Figure 21. Tower profile plots from 2300 UTC 10 August (green), 0000 UTC (purple), 0100 UTC (blue), and 0200 UTC 11 August (red). The solid lines are the temperature profiles and the dashed lines are the associated dew point temperature profiles.

MESOSCALE MODELING

Weather Research and Forecasting (WRF) Model Sensitivity Study (Dr. Watson)

The WRF model is the next generation community mesoscale model designed to enhance collaboration between the research and operational sectors. The SMG and the NWS MLB are moving forward with implementing the WRF model operationally into their AWIPS systems. The WRF model has two dynamical cores – the Advanced Research WRF (ARW) and the Non-hydrostatic Mesoscale Model (NMM). There are also two options for the initialization of the WRF model – the Local Analysis and Prediction System (LAPS) and the Advanced Regional Prediction System (ARPS) Data Analysis System (ADAS). Having a series of initialization options and WRF cores, as well as many options within each core, provides SMG and NWS MLB with a lot of flexibility as well as challenges. This includes determining which configuration options are best to address specific forecast concerns. The goal of this task to assess the different configurations available and to determine which configuration will best predict warm season convective initiation. To accomplish this, the AMU was tasked to

- Compare the WRF model performance using ADAS versus LAPS for the ARW and NMM model cores,
- Compare the impact of using a high-resolution local forecast grid with 2-way, 1-way, and no nesting, and
- Examine the impact of assimilating soil moisture sensor data on WRF model performance.

Model Verification

Dr. Watson completed the precipitation verification for all model initializations and nesting options within the WRF model. To verify precipitation, she compared the hourly forecast rainfall accumulation to the National Centers for Environmental Prediction (NCEP) stage-IV precipitation analysis. To determine the skill of each model configuration, she employed the Fractions Skill Score (FSS). The FSS is an objective precipitation verification method based on the Brier Skill Score that answers the question of what spatial scales the forecast resembles the observations (Roberts 2005).

Figure 22 shows the forecast bias for the ADAS-ARW configuration. Dr. Watson ran this configuration using a 4-km grid over the Florida peninsula and surrounding waters. It is apparent in Figure 22 that this configuration consistently over-predicted rainfall accumulation throughout the forecast period, but failed to capture the late afternoon convective maximum. The figure also shows a sharp increase in rainfall accumulation within the first two hours of the forecast. This indicates a model spin-up issue even with a hot-start initialization.

Figure 23 shows the results from the calculation of FSS for ADAS-ARW. The calculation compares the model to the NCEP stage-IV precipitation analysis for five different spatial scales from 4 to 160 km. The FSS values range from 0 to 1, where 1 indicates a perfect forecast and 0 indicates no skill. The ADAS-ARW showed the least skill two hours after model initialization. This was consistent with the time of the maximum precipitation bias and also due to the model spin up issue. This configuration showed some skill at predicting warm season convection in the 6–12 hour range over the spatial scales of 40 to 160 km.

Figure 24 shows the forecast bias for the LAPS-ARW one-way nesting configuration. Dr. Watson ran the one-way nest was run using a 1.33-km grid centered over east-central Florida. This configuration over-predicted precipitation during the initial stages of the forecast, exhibiting the same model spin up problem as was seen with the ADAS-ARW run. The configuration captured the timing of the late afternoon convective maximum, although it under-predicted the rainfall during this time. The timing of the late afternoon convective maximum in the 1500 UTC runs of the nesting configuration was delayed by approximately three hours.

Figure 25 shows the results from the calculation of FSS for the one-way nest. The calculation compares the model to the stage-IV precipitation analysis for five different spatial scales from 1.3 to 53.2 km. The FSS indicates low skill with values of 0.3–0.4 during the first few hours, increasing to 0.4–0.6 in the last five hours with peak skill at the 8-hour forecast. This configuration increased in skill by nearly 50% from the first six hours of the forecast to the last six hours. This suggests that the model still had a problem with spin up even when running at a higher resolution on a smaller domain.

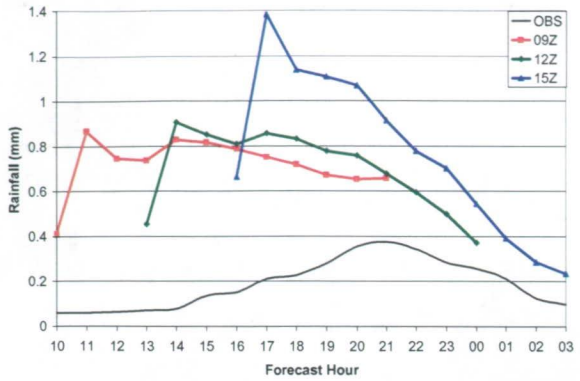

Figure 22. The bias of rainfall accumulation (mm) versus forecast hour (UTC) for ADAS-ARW. The black line is the hourly observed rainfall accumulation averaged over the 4-km domain. The red, green, and blue lines are the averaged forecast rainfall accumulations for all model runs initialized at 0900, 1200, and 1500 UTC, respectively.

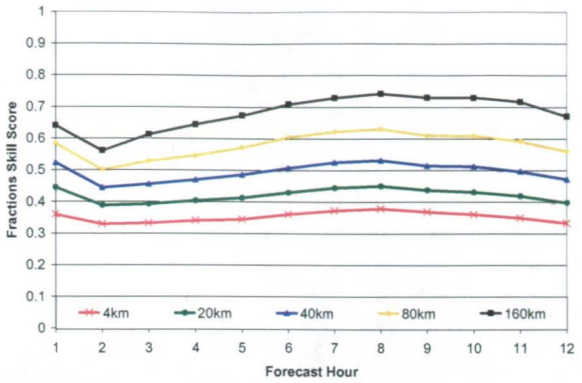

Figure 23. The FSS versus forecast hour (UTC) for ADAS-ARW. The colors represent model skill on different spatial scales, from the grid scale at 4-km to 160-km. The color legend is on the bottom of the chart.

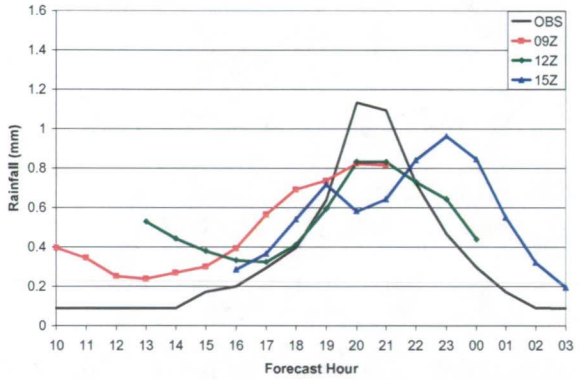

Figure 24. The bias of rainfall accumulation (mm) versus forecast hour (UTC) for the LAPS-ARW 1.33-km nest using one-way nesting. The black line is the hourly observed rainfall accumulation averaged over the 1.33-km domain. The red, green, and blue lines are the averaged forecast rainfall accumulations for all model runs initialized at 0900, 1200, and 1500 UTC, respectively.

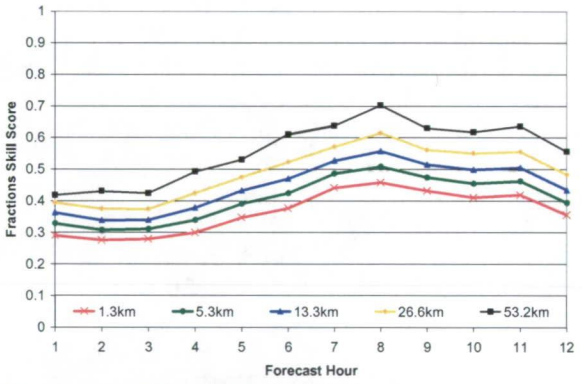

Figure 25. The FSS versus forecast hour for the LAPS-ARW 1.33-km nest using one-way nesting. The colors represent model skill on different spatial domains, from the grid scale of 1.33-km to 53.2-km. The color legend is on the bottom of the chart.

Soil Moisture Assimilation

Currently, ADAS cannot assimilate in situ soil moisture data into its analysis. Therefore, in the original task the AMU determined that sensitivity tests involving soil moisture would have to be conducted using LAPS. After further research, Dr. Watson found that LAPS was also unable to assimilate soil moisture data due to the way in which the software is currently written for three reasons:

1) The LAPS soil moisture algorithm provides a three-layer analysis of soil moisture and does not provide a soil temperature analysis. The WRF Environmental Modeling System (EMS) software requires input of soil moisture and temperature data on at least four levels. This code was written such that if less than four layers of soil data were available from LAPS, it would not be used.

2) Soil moisture data at KSC are available at a depth of 3 cm, integrated over 3 to 10 cm, and integrated over 38 to 76 cm below the surface. LAPS only ingests one level of soil moisture data, but the level needed is not specified anywhere in the code.
3) LAPS does not use any soil moisture data in the soil moisture algorithm, nor does it use the soil moisture data for deriving any other atmospheric variable.

Currently, the use of a Land Data Assimilation Scheme (LDAS) is the only way to incorporate soil moisture data into the WRF model. One LDAS currently available to the public is NASA's Land Information System (LIS). This system runs several different land surface models (LSM) using model and observational input, including precipitation and many surface parameters.

Conclusions and Final Report

The major results from the study showed the following.

- Both the ADAS-ARW and LAPS-ARW configurations developed too much precipitation across the forecast area during the model spin up period and over-predicted rainfall amounts across the forecast area throughout the 12-hour forecast.
- Based on a subjective analysis of the three WRF initializations, LAPS-ARW slightly outperformed the other two configurations.
- Both one- and two-way nesting configurations under-predicted the late afternoon convective maximum over east-central Florida.
- The difference in skill between the one-way, two-way, and no nest configurations was negligible.
- As the forecast progressed in all WRF initializations and nesting configurations, the rainfall bias decreased and the skill increased, indicating that all models performed better beyond six hours.
- The use of a local high-resolution grid did not significantly improve the skill of the model as compared to the 4 km model runs.

The analysis of all hot-start model and nesting configurations indicated that no single model was better than the rest. These results suggest that high-resolution forecasts over Florida during the warm season are best to help develop a broad understanding of a convective event rather than in predicting individual convective cells.

Of the three model configurations tested, the AMU recommended the LAPS-ARW configuration for operational use for predicting warm season convective initiation for the following reasons:

- Although the FSS for the LAPS-ARW and ADAS-ARW forecasts were nearly identical, LAPS-ARW appeared to over-predict the precipitation less than ADAS-ARW;
- The LAPS-NMM configuration produced forecasts that were too dry;
- The ADAS does not have the capability to assimilate soil moisture data, but a soil moisture algorithm is being developed for LAPS; and
- The challenge of setting up the LAPS software can be avoided by using LAPS analyses from AWIPS for use within the WRF EMS software, eliminating the need for running an outside analysis before running the WRF model.

Dr. Watson presented the findings from this study at the 22nd Conference on Weather Analysis and Forecasting/18th Conference on Numerical Weather Prediction held in Park City, Utah from June 25 – 29, 2007. She completed a first draft of the final report and submitted it for internal AMU and external customer review.

For more information, contact Dr. Watson at watson.leela@ensco.com or 321-853-8264.

AMU CHIEF'S TECHNICAL ACTIVITIES (Dr. Merceret)

Dr. Merceret conducted an analysis of additional cases of clear-air electric fields associated with anvil and debris cloud as requested by the Lightning Advisory Panel. He also wrote the first draft of a journal manuscript presenting the coherence and correlation results from his 2006 study of spatial properties of winds in the lowest 3 km of the atmosphere and sent it to a colleague for internal review.

AMU OPERATIONS

Tasking Meeting

All AMU team members participated in the annual AMU Tasking Meeting held on 24 April in the ENSCO Cocoa Beach office. Six new tasks were assigned for the coming year:

1) Impact of Local Sensors is meant to determine the impact of reducing the number wind towers and daily rawinsonde launches using a high resolution model;
2) RadTec Radar Scan Strategy, Phase I will develop new scan strategies for the new radar planned to replace the WSR-74C at Patrick AFB;
3) Objective Lightning Probability Tool, Phase III will create new forecast equations based on new stratifications and an expanded warm season.
4) Situational Lightning Climatology for Central Florida, Phase III will incorporate the climatological soundings based on flow regime into AWIPS;
5) AWIPS Anvil Forecast Tool, Phase II will add new functionality to the current tool; and
6) WRF Wind Sensitivity Study for Edwards AFB will determine the best WRF configuration to forecast the surface wind field.

General

Mr. Barrett worked on several issues with the NASA Procurement office concerning orders and sole-source justifications. He wrote a sole-source justification for the ESRI ArcView GIS software, and Ms. Lambert wrote a sole-source justification for S-PLUS with the help of Dr. Merceret. Mr. Barrett and Dr. Bauman responded to a request by NASA to list the AMU's computer servers. A goal of NASA's Agency Office of the Chief Information Officer is to consolidate data centers throughout NASA, and to host computer services from facilities that provide adequate security, administration, availability, reliability and disaster recovery capabilities in an efficient manner. Dr. Bauman and Ms. Lambert met with Ms. Kathy Futch of the 45th Security Forces Squadron to conduct the AMU's annual security inspection.

Dr. Bauman distributed a memorandum describing an issue with the XMR soundings transmitted through NOAAPort. There is an algorithm in the software at CCAFS that changes the dew point depression to 30° C when the relative humidity is 20% or less at any level. This algorithm was a requirement over 30 years ago, but it has since been removed. The memorandum advises that the data archived at Weather Station A and CSR should be used in studies until CSR is able to remove that line of code.

Launch Support

Ms. Lambert supported the STS-117 launch, Mr. Wheeler supported the Atlas V launch, and Mr. Barrett supported the STS-117 landing.

Conferences and Meetings

Dr. Bauman, Ms. Lambert, and Mr. Barrett each submitted abstracts for the 37th Annual Meeting of the National Weather Association to be held in Reno, Nevada in October 2007. The abstract titles are "Flow Regime-Based Climatologies of Lightning Probabilities for Spaceports and Airports", "Update to the Lightning Probability Forecast Equations at Kennedy Space Center/Cape Canaveral Air Force Station, Florida", and "Creating Interactive Graphical Overlays in the Advanced Weather Interactive Processing System Using Shapefiles and DGM Files", respectively.

Dr. Watson attended the 22nd Conference on Weather Analysis and Forecasting / 18th Conference on Numerical Weather Prediction held 25–29 June in Park City, Utah. She presented results from the WRF Model Sensitivity task.

Dr. Bauman chaired the Short-term Prediction Research and Transition Center (SPoRT) Science Advisory Council meeting in Huntsville, AL from 12–14 June.

Dr Short Sabbatical Notes

Dr. Short began a four-month sabbatical at Nagoya University in Japan on 1 April. The goal of his work is to look closely at shallow convective rain from the Tropical Rainfall Measuring Mission (TRMM) precipitation radar (PR) in an attempt to improve rainfall rate retrieval algorithms and to improve knowledge of small-scale boundary layer convection over the tropical oceans.

Dr. Short looked at shallow convective rain cases in TRMM data collected during June, July and August 1998–2000. He obtained a database of about 60,000 observations from the PR over the central Pacific Inter-Tropical Convergence Zone (ITCZ) and the marine stratocumulus area

west of South America. He also collected TRMM data from the post-boost phase, when the TRMM satellite altitude was increased from 350 to 400 km in August 2001 to increase mission life. The increased altitude resulted in an increase of the radar field-of-view (FOV) from 4.3 to 5.0 km, and he looked at the impact of the increased FOV on statistics of shallow, isolated convection.

From his analysis, Dr. Short developed a simple rain cell model and tuned it to match statistics of radar reflectivity from shallow isolated convection that was observed by the TRMM Radar over the central Pacific ITCZ. By assuming an aspect ratio (cell diameter divided by cell depth) of two and a cloud base height of 500 m, the model and TRMM PR show reasonable agreement (Figure 26). The model can also be used to estimate rainfall rate retrieval errors due to incomplete beam-filling.

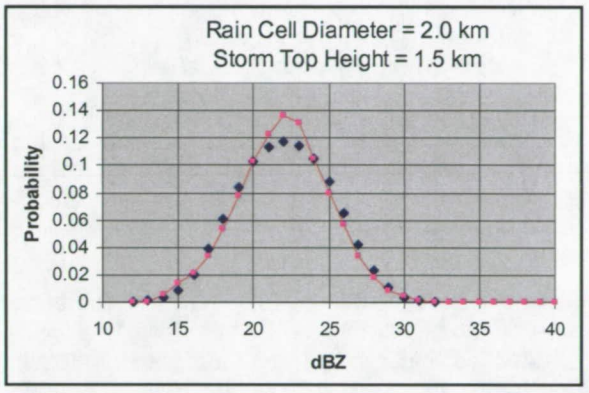

Figure 26. Probability distributions of radar reflectivity (dBZ) observed by the TRMM PR for shallow isolated convection with tops at 1.5 km over the central Pacific ITCZ (pink curve) and calculated from an idealized model with circular rain cells with diameters of 2 km (blue diamonds).

Dr. Short gave two presentations on this work while in Japan. The first was for the Nagoya University Laboratory of Satellite Meteorology weekly colloquium and the second was in Tokyo at the National Institute for Information and Communications Technology.

Plymouth State University Visitors

Dr. James Koermer and two students from Plymouth State University (PSU), Heather Dinon and Matthew Morin, arrived in the AMU on 6 June to conduct research for the 45 WS. Mr. Barrett set up two new computer user accounts and computers for the students prior to their arrival.

Dr. Koermer obtained support for himself and the two students from the NASA Space Grant Program to conduct research on convective winds for the KSC/CCAFS area. They will be in the AMU until 10 August. Their research this year will be in the following areas:

- Update the PSU web page on KSC/CCAFS convective winds:
  (http://vortex.plymouth.edu/conv_winds/)
- Fine-tune the convective climatology that was developed over the last two summers using newly acquired archived Weather Surveillance Radar 1988 Doppler (WSR-88D) data for MLB and Tampa (TBW) and new radar display capabilities.
- Continue to investigate the peak wind "lead time" issue, based on earlier preliminary results showing considerable ramp up time (30 minutes or more) of peak wind speeds for about two-thirds of the convective events.
- Expand the investigation of thermodynamic parameters to include all convective events during the warm-seasons of 1995-2005.
- Initiate a new study to see what the loss of some towers in the network would do to convective wind predictability.

They finished the initial update of the PSU Convective Wind web page, downloaded WSR-88D data for MLB and TBW covering more than 800 convective periods, and developed a radar visualization tool with high zoom capability that overlays the KSC/CCAFS wind tower locations (Figure 27).

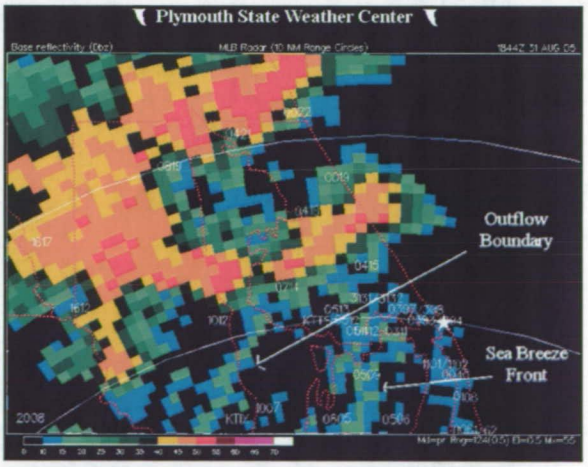

Figure 27. The new PSU radar display used for analysis of convective peak winds. The tower number are overlain on the radar data.

REFERENCES

Barrett, J. H., and W. H. Bauman, 2007: Anvil Tool in the Advanced Weather Interactive Processing System. NASA Contractor Report CR-2007-214729, Kennedy Space Center, FL, 26 pp. [Available from ENSCO, Inc., 1980 N. Atlantic Ave., Suite 230, Cocoa Beach, FL 32931 and online at http://science.ksc.nasa.gov/amu/final.html.]

Bauman, W. H., 2007: Users Guide for the Anvil Threat Corridor Forecast Tool V1.7.0 for AWIPS. AMU user guide, 29 pp. [Available from ENSCO, Inc., 1980 N. Atlantic Ave., Suite 230, Cocoa Beach, FL 32931 and online at http://science.ksc.nasa.gov/amu/final.html.]

Dye, J. E., M. G. Bateman, D. M. Mach, C. A. Grainger, H. J. Christian, H. C. Koons, E. P. Krider, F. J. Merceret, and J. C. Willett, 2006: The scientific basis for a radar-based lightning launch commit criterion for anvil clouds. Preprint 8.4, 12th Conf. on Aviation, Range, and Aerospace Meteorology, Atlanta, GA, Amer. Meteor. Soc., 4 pp. [Available online at: http://ams.confex.com/ams/pdfpapers/100563.pdf]

Dye, J. E., M. G. Bateman, H. J. Christian, E. Defer, C. A. Grainger, W. D. Hall, E. P. Krider, S. A. Lewis, D. M. Mach, F. J. Merceret, J. C. Willett, and P. T. Willis, 2007: Electric fields, cloud microphysics and reflectivity in anvils of Florida thunderstorms, *J. Geophys. Res.*, **112**, D11215, doi10.1029/2006JD007550.

Dye, J.E., S. Lewis, M.G. Bateman, D.M. Mach, F.J. Merceret, J.G. Ward and C.A. Grainger, 2004: Final Report on the Airborne Field Mill Project (ABFM) 2000-2001 Field Campaign, NASA Technical Memorandum NASA/TM-2004-211534, November 2004, 132 pp.

Felsch, P., 1993: Stratus Surge Prediction along the Central California Coast. *Wea. Forecasting*, **8**, 204–213.

Lambert, W., D. Sharp, S. Spratt, and M. Volkmer, 2006: Using Cloud-to-Ground Lightning Climatologies to Initialize Gridded Lightning Threat Forecasts for East Central Florida. Preprints, *Second Conf. on Meteorological Applications of Lightning Data,* Paper 1.3, Atlanta, GA, Amer. Meteor. Soc., 4 pp.

Lambert, W. and M. Wheeler, 2005: Objective Lightning Probability Forecasting for Kennedy Space Center and Cape Canaveral Air Force Station. NASA Contractor Report CR-2005-212564, Kennedy Space Center, FL, 54 pp. [Available from ENSCO, Inc., 1980 N. Atlantic Ave., Suite 230, Cocoa Beach, FL 32931 and http://science.ksc.nasa.gov/amu/final.html.]

Lericos, T. P., H. E. Fuelberg, A. I. Watson, and R. L. Holle, 2002: Warm season lightning distributions over the Florida Peninsula as related to synoptic patterns. *Wea. Forecasting*, **17**, 83 – 98.

Roberts, N. M., 2005: An investigation of the ability of a storm-scale configuration of the Met Office NWP model to predict flood-producing rainfall. *Forecasting Research Tech. Rept. 455,* Met Office, 80 pp.

Short, D., 2006: Situational Lightning Climatologies for Central Florida, Phase II. Applied Meteorology Unit Memorandum, 8 pp. [Available from ENSCO, Inc., 1980 N. Atlantic Ave., Suite 230, Cocoa Beach, FL 32931]

Wells, L., 2005: Marine Layer Stratus Study, 30th Weather Squadron Field Memorandum, FM-05/001, 37 pp. [Available from 30 WS, 900 Corral Road, Bldg. 21150, VAFB, CA 93437-5002]

Willett, J. C., H. C. Koons, E. P. Krider, R. L. Walterscheid, and W. D. Rust, 1999: Natural and Triggered Lightning Launch Commit Criteria (LLCC), Aerospace Report A923563, Aerospace Corp., El Segundo, CA, 23 pp.

List of Acronyms

30 SW	30th Space Wing
30 WS	30th Weather Squadron
45 RMS	45th Range Management Squadron
45 OG	45th Operations Group
45 SW	45th Space Wing
45 SW/SE	45th Space Wing/Range Safety
45 WS	45th Weather Squadron
ADAS	ARPS Data Analysis System
AFSPC	Air Force Space Command
AFWA	Air Force Weather Agency
AMU	Applied Meteorology Unit
ARPS	Advanced Regional Prediction System
ARW	Advanced Research WRF
AWIPS	Advanced Weather Interactive Processing System
CB	ENSCO Cocoa Beach Office
CCAFS	Cape Canaveral Air Force Station
CG	Cloud-to-Ground Lightning
CSR	Computer Sciences Raytheon
DAB	Daytona Beach 3-letter identifier
EMS	Environmental Modeling System
EST	Eastern Standard Time
FOV	Field of View
FPR	St. Lucie, FL 3-letter identifier
FR	Flight Rules
FSS	Fraction Skill Score
FSU	Florida State University
FY	Fiscal Year
GSD	Global Systems Division
GUI	Graphical User Interface
HTML	Hypertext Markup Language
ISM	Kissimmee, FL 3-letter identifier
ITCZ	Intertropical Convergence Zone
JSC	Johnson Space Center
KSC	Kennedy Space Center
LAPS	Local Analysis and Prediction System
LCC	Launch Commit Criteria
LEE	Leesb Leesburg, FL 3-letter identifier
LLCC	Lightning LCC
MAE	Mean Absolute Error
MCO	Orlando, FL 3-letter identifier
MIDDS	Meteorological Interactive Data Display System
MLB	Melbourne, FL 3-letter identifier
MSFC	Marshall Space Flight Center
MSL	Mean Sea Level
NASA	National Aeronautics and Space Administration
NCAR	National Center for Atmospheric Research
NCEP	National Centers for Environmental Prediction
NMM	Non-hydrostatic Mesoscale Model
NOAA	National Oceanic and Atmospheric Administration
NSSL	National Severe Storms Laboratory
NWS	National Weather Service
NWS MLB	NWS in Melbourne, FL
ORPG	Open Radar Product Generator
PR	Precipitation Radar on TRMM
PSU	Plymouth State University
QC	Quality Control
R^2	Coefficient of Determination
RH	Relative Humidity
RSA	Range Standardization and Automation
SFB	Sanford, FL 3-letter identifier
SLF	Shuttle Landing Facility
SMC	Space and Missile Center
SMG	Spaceflight Meteorology Group
SPoRT	Short-term Prediction Research and Transition
TBW	Tampa, FL 3-letter identifier
Tcl/Tk	Tool Command Language/Toolkit
TRMM	Tropical Rainfall Measuring Mission
USAF	United States Air Force
UTC	Universal Coordinated Time
VAFB	Vandenberg Air Force Base
VAHIRR	Volume Averaged Height Integrated Radar Reflectivity
VRB	Vero Beach, FL 3-letter identifier
VBG	VAFB 3-letter identifier
WRF	Weather Research and Forecasting Model
WSR-88D	Weather Surveillance Radar 1988 Doppler
XMR	CCAFS 3-letter identifier

Appendix A

AMU Project Schedule 31 July 2007				
AMU Projects	Milestones	Scheduled Begin Date	Scheduled End Date (*New End Date*)	Notes/Status
Objective Lightning Probability Phase II	Calculate new forecast parameters	Jan 06	Feb 06 (*Oct06*)	Completed Delayed due to delays in Lightning Climatology task
	Develop and test new equations	Mar 06	Apr 06 (*Feb 07*)	Completed Delayed as above
	Update the MIDDS tool with new equations	Apr 06	Apr 06 (*Jun 07*)	Completed Delayed as above
	Final report	Mar 06	May 06 (*Jul 07*)	Delayed as above
Peak Wind Tool for General Forecasting	Data collection: wind towers, XMR 100-ft soundings, 915-MHz profilers	Sep 06	Oct 06 (*Feb 07*)	Completed Delayed to obtain 915-MHz profiler data
	Software development: wind tower data QC, sounding inversion detection, 915 MHz total power display	Sep 06	Dec 06 (*Mar 07*)	Completed Delayed to modify the AMU wind tower QC software
	Data analysis	Dec 06	Feb 07 (*Jun 07*)	Completed Delayed to add recent data sets
	Interim evaluation	Feb 07	Mar 07	Completed
	Forecast tool development, if approved	Mar 07	May 07 (*Jul 07*)	Delayed as above
	Final report	Jun 07	Jul 07	On Schedule
Situational Lightning Climatologies for Central Florida: Phase II	Modify code and develop algorithms needed to create climatologies	Nov 06	Mar 07	Completed
	Calculate number of lightning strikes in all boxes and output one value for each circle size for each flow regime	Mar 07	May 07	Completed
	Final memorandum	May 07	Jun 07 (*Jul 07*)	Delayed due to extended customer review of GUI

AMU Project Schedule 31 July 2007				
AMU Projects	Milestones	Scheduled Begin Date	Scheduled End Date (*New End Date*)	Notes/Status
Anvil Forecast Tool in AWIPS	AWIPS training at GSD	Jul 05	Nov 05 (*Jan 07*)	Completed Delayed due to funds transfer issues
	Develop software for calculation and display of anvil threat corridor	Dec 05	Apr 06 (*Oct 06*)	Completed Delayed due to delay in training
	Test and evaluate performance of the software	Apr 06	May 06 (*Mar 07*)	Completed Delayed as above
	Final memorandum	May 06	June 06 (*May 07*)	Completed Delayed as above
Volume-Averaged Height Integrated Radar Reflectivity (VAHIRR)	Acquisition and setup of development system and preparation for Technical Advisory Committee meeting	Mar 05	Apr 05	Completed
	Software Recommendation and Enhancement Committee meeting preparation	Apr 05	Jun 05	Completed
	VAHIRR algorithm development	May 05	Oct 05 (*Jul 06*)	Completed – Delayed due to new code development made necessary by final product requirements
	ORPG documentation updates	Jun 05	Oct 05 (*Sep 06*)	Completed Delayed as above
	Configure ORPG and AWIPS system in the AMU for live data testing.	Oct 05	Jan 06 (*Aug 07*)	Delayed as above
	Preparation of products for delivery and memorandum	Oct 05	Jan 06 (*Sep 07*)	Delayed as above
Subtask 26: Tower Data Skew-T Tool	Data collection: RSA wind towers, VBG soundings, VBG ASOS observations	Mar 07	Apr 07	Completed
	Data analysis, case study review using the 30 WS Tower Data Skew-T Tool	Apr 07	Jul 07	On Schedule
	Memorandum and presentation to 30 WS	Aug 07	Aug 07	On Schedule

AMU Project Schedule 31 July 2007				
AMU Projects	Milestones	Scheduled Begin Date	Scheduled End Date (*New End Date*)	Notes/Status
WRF Model Sensitivity Tests	Identify candidate convective initiation days and archive data	Jul 06	Sep 06	Completed
	Configure LAPS to initialize WRF	Aug 06	Oct 06 (*Feb 07*)	Completed Delayed due to satellite data conversion issues
	Compare LAPS-WRF vs. ADAS-WRF performance	Aug 06	Jan 07 (*May 07*)	Completed Delayed as above
	Compare use of high-resolution grid with 2-way, 1-way, and no nesting	Jan 07	Mar 07 (*May 07*)	Completed Delayed as above
	Assess impact of soil moisture data on WRF performance	Feb 07	Apr 07 (*May 07*)	Completed Delayed as above
	Final report and recommendations	Apr 07	Jun 07 (*Jul 07*)	Delayed as above

NOTICE

Mention of a copyrighted, trademarked, or proprietary product, service, or document does not constitute endorsement thereof by the author, ENSCO, Inc., the AMU, the National Aeronautics and Space Administration, or the United States Government. Any such mention is solely for the purpose of fully informing the reader of the resources used to conduct the work reported herein.